9-7-2013

Synthesis, Characterisation, and Preliminary Anti-Cancer Photodynamic Therapeutic *In Vitro* Studies of Mixed-Metal Binuclear Ruthenium(II)-Vanadium(IV) Complexes

Alvin A. Holder
University of Southern Mississippi, aholder@odu.edu

Patrick Taylor
University of Southern Mississippi

Anthony R. Magnusen
University of Southern Mississippi

Erick T. Moffett
University of Southern Mississippi, erick.moffett@usm.edu

Kyle Meyer
University of Dayton

See next page for additional authors

Published in final edited form as:
Dalton Trans. 2013 September 7; 42(33): 11881–11899. doi:10.1039/c3dt50547b.

Synthesis, characterisation, and preliminary anti-cancer photodynamic therapeutic *in vitro* studies of mixed-metal binuclear ruthenium(II)-vanadium(IV) complexes

Alvin A. Holder[a], **Patrick Taylor**[a], **Anthony R. Magnusen**[a], **Erick T. Moffett**[a], **Kyle Meyer**[b], **Yiling Hong**[b], **Stuart E. Ramsdale**[a], **Michelle Gordon**[a], **Javelyn Stubbs**[a], **Luke A. Seymour**[a], **Dhiraj Acharya**[c], **Ralph T. Weber**[d], **Paul F. Smith**[e], **G. Charles Dismukes**[e], **Ping Ji**[f], **Laura Menocal**[f], **Fengwei Bai**[c], **Jennie L. Williams**[f], **Donald M. Cropek**[g], and **William L. Jarrett**[h]

[a]Department of Chemistry and Biochemistry, The University of Southern Mississippi, 118 College Drive, # 5043, Hattiesburg, Mississippi 39406-0001, U.S.A. alvin.holder@usm.edu, telephone: 601-266-4767, and fax: 601-266-6075

[b]Department of Biology, University of Dayton, 300 College Park, Dayton, OH 45469-2320, U.S.A.

[c]Department of Biological Sciences, The University of Southern Mississippi, MS 39406, U.S.A.

[d]EPR Division Bruker BioSpin, 44 Manning Road, Billerica, MA 01821, U.S.A.

[e]Department of Chemistry and Chemical Biology, Rutgers, The State University of New Jersey, Piscataway, NJ 08854, U.S.A.

[f]Department of Medicine, Stony Brook University, HSC T-17 room 080, Stony Brook, NY 11794-8175, U.S.A.

[g]U.S. Army Corps of Engineers, Construction Engineering Research Laboratory, Champaign, IL 61822, U.S.A.

[h]School of Polymers and High-Performance Materials, The University of Southern Mississippi, 118 College Drive, #5050, Hattiesburg, MS 39406-0076, U.S.A.

Abstract

We report the synthesis and characterisation of mixed-metal binuclear ruthenium(II)-vanadium(IV) complexes, which were used as potential photodynamic therapeutic agents for melanoma cell growth inhibition. The novel complexes, $[Ru(pbt)_2(phen_2DTT)](PF_6)_2 \cdot 1.5H_2O$ **1** (where $phen_2DTT$ = 1,4-bis(1,10-phenanthrolin-5-ylsulfanyl)butane-2,3-diol and pbt = 2-(2'-pyridyl)benzothiazole) and $[Ru(pbt)_2(tpphz)](PF_6)_2 \cdot 3H_2O$ **2** (where tpphz = tetrapyrido[3,2-*a*:2′, 3′-*c*:3″,2″-*h*:2‴,3‴-*j*]phenazine) were synthesised and characterised. Compound **1** was reacted with [VO(sal-*L*-tryp)(H_2O)] (where sal-*L*-tryp = *N*-salicylidene-*L*-tryptophanate) to produce $[Ru(pbt)_2(phen_2DTT)VO(sal\text{-}L\text{-}tryp)](PF_6)_2 \cdot 5H_2O$ **4**; while [VO(sal-*L*-tryp)(H_2O)] was reacted

Correspondence to: Alvin A. Holder.

†Electronic Supplementary Information (ESI) available: Figures featuring ESI MS (Figs. S1–S4), FT IR spectra (Fig. S5), X-band ESR spectra (Fig. S6), UV-visible spectrum of $Na_4[Co(tspc)(H_2O)_2]$ (Fig. S7), phase-contrast microscope images (Fig. S8), and FT IR data (Table 1) are collated here. See DOI: 10.1039/b000000x/

with compound **2** to produce $[Ru(pbt)_2(tpphz)VO(sal\text{-}L\text{-}tryp)](PF_6)_2 \cdot 6H_2O$ **3.** All complexes were characterised by elemental analysis, HRMS, ESI MS, UV-visible absorption, ESR spectroscopy, and cyclic voltammetry, where appropriate. *In vitro* cell toxicity studies (with the 3-(4,5-dimethylthiazol-2-yl)-2,5-diphenyltetrazolium bromide (MTT) colorimetric assay) via dark and light reaction conditions were carried out with sodium diaqua-4,4',4”, 4”'tetrasulfophthalocyaninecobaltate(II) ($Na_4[Co(tspc)(H_2O)_2]$), $[VO(sal\text{-}L\text{-}tryp)(phen)] \cdot H_2O$, and the chloride salts of complexes **3** and **4**. Such studies involved A431, human epidermoid carcinoma cells; human amelanotic malignant melanoma cells; and HFF, non-cancerous human skin fibroblast cells. Both chloride salts of complexes **3** and **4** were found to be more toxic to melanoma cells than to non-cancerous fibroblast cells, and preferentially led to apoptosis of the melanoma cells over non-cancerous skin cells. The anti-cancer property of the chloride salts of complexes **3** and **4** was further enhanced when treated cells were exposed to light, while no such effect was observed on non-cancerous skin fibroblast cells. ESR and ^{51}V NMR spectroscopic studies were also used to assess the stability of the chloride salts of complexes **3** and **4** in aqueous media at pH 7.19. This research illustrates the potential for using mixed-metal binuclear ruthenium(II)-vanadium(IV) complexes fighting skin cancer.

Introduction

Malignant melanoma is a tumour that arises from melanocytes or from cells that develop from melanocytes. In 2010, approximately 68,130 new cases of melanoma were diagnosed, of which 8,700 patients (approximately 12.8%) died of this disease in the United States.[1] In 2012, it was estimated that 9,180 men and women died from malignant melanoma in the U.S.A.[2] Cisplatin is widely used for the treatment of many cancers (including malignant melanoma)[3] despite its high toxicity, undesirable side effects, and problems with drug resistance in primary and metastatic cancers.[4, 5] Due to these limitations, there is a steadily growing interest in novel non-platinum metal complexes that show anti-cancer properties.[6] Also, it has been found that metastatic melanoma is highly resistant to chemotherapy, radiation therapy, hormonal therapy, and modern immunotherapeutic approaches; hence there is a need to find new efficient approaches to treat melanoma. One treatment combination that might be effective would combine an organometallic compound as a chemotherapeutic agent with a photosensitizing agent followed by laser destruction of cancer using photodynamic therapy (PDT).[7] Mechanistically, PDT uses light, molecular oxygen, and a photosensitizer to induce cell death,[7] whereby reactive oxygen species (ROS) such as singlet oxygen and radical species are the deleterious agents responsible for cell death.[8] Research on the use of PDT is focused on developing photosensitizers that show little or no dark toxicity, concentrate at tumour sites, and can create ROS indirectly through long wavelength illumination. Photofrin, an FDA approved photosensitizer,[9–11] has been proven to generate singlet oxygen from triplet oxygen through energy transfer upon photoexcitation in the visible region of the spectrum resulting in cell death.[9–11] Due to the fact that Photofrin also suffers from dark toxicity and purification difficulties,[9–12] it is imperative to find a suitable replacement that eliminates such negative attributes.

For some time now, many metal complexes have been shown to exhibit light-activated reactions with DNA.[10, 13, 14] It has been reported that ruthenium-containing complexes do

possess several favourable properties suited to rational anti-cancer drug design,[14–16] since these complexes can reduce tumour growth by interaction with DNA and RNA, although non-genomic targets also appear to be important, such as transferrin, which allows them to be selectively transported into cancer cells.[17–20] Most research has focused on ruthenium(III) and to a lesser extent ruthenium(IV) complexes, although some recent studies using organometallic ruthenium(II) arene compounds have shown considerable promise for the treatment of cancer and metastasis.[21, 22] Some ruthenium(III) complexes have been actively studied as metallodrugs as they are believed to have low toxicity and good selectivity for tumours.[23] It has been reported that two ruthenium(III) compounds, viz., NAMI-A and KP1019, developed by Gianferrara and co-workers, and by the group of Keppler, respectively, have been successful anti-cancer agents.[23–25] KP1019 and NAMI-A have successfully completed phase 1 clinical trials; NAMI-A entered phase 2 clinical trials in 2008 (in combination with a cytotoxic drug), and KP1019 is about to be used in chemotherapy.[26] Both compounds were reported to be moderately cytotoxic *in vitro* and, in animal models, were found to have activities different from established platinum-containing drugs. NAMI-A was found to be particularly active against the development and growth of metastases of solid tumours,[27] whereas KP1019 has been shown to exhibit excellent activity against platinum-resistant colorectal tumours.[24, 25]

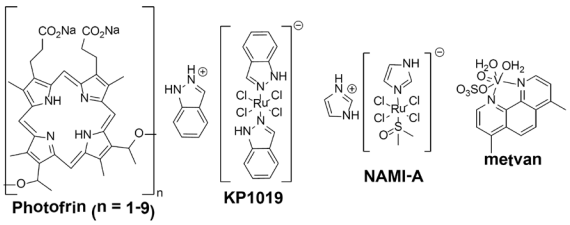

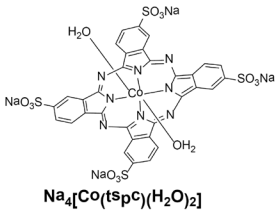

Holder *et al*.[28, 29] have recently published findings on the first generation supramolecular complexes $[((bpy)_2M(dpp))_2RhCl_2]Cl_5$ (where dpp = 2,3-bis(2-pyridyl)pyrazine, bpy = 2,2'-bipyridine, and M = Os, Ru)), that photocleave DNA and photochemically inhibit cell division. Ruthenium complexes coordinated to the periphery of porphyrin molecules have also been reported to interact with DNA.[30, 31] A separate study of a tetraruthenated porphyrin suggested electrostatic binding to DNA and photocleavage of circular plasmid DNA through formation of singlet oxygen.[32] Schmitt *et al*.[33] have also reported a study of ruthenium porphyrin compounds for PDT of human melanoma tumour cells, while Gianferrara *et al*.[34] reported the *in vitro* cell growth inhibition of MDA-MB-231 human breast cancer cells and HBL-100 human non-tumourigenic epithelial cells by ruthenium(II)-

porphyrin conjugates. It must also be mentioned that Rani-Beeram *et al*.[35] reported studies involving a fluorinated ruthenated porphyrin as a potential PDT agent through DNA and melanoma cell studies where they reported that the ruthenated porphyrin was more toxic to melanoma skin cells than those of non-cancerous fibroblast cells when irradiated with a 60 W tungsten lamp.

More recently, Higgins *et al*.[36] reported metal-to-ligand charge transfer induced DNA photobinding in a Ru(II)–Pt(II) supramolecule using red light in the therapeutic window. Just around that time, Wachter *et al*.[37] reported that incorporation of biquinoline ligands into ruthenium(II) polypyridyl complexes produced light-activated systems that ejected a ligand and photobind DNA after irradiation with visible and NIR light. It was reported that structural analysis showed that distortion facilitated the photochemistry; while gel shift and cytotoxicity studies proved the compounds acted as anti-cancer PDT agents in the tissue penetrant region.[37] Of note, a recent review written by Chakravarty and Roy[38] is focused on photoactivated DNA cleavage and anti-cancer activity involving 3d metal complexes.

Researchers have also reported extensive studies of the cleavage of DNA with vanadium-containing complexes, inclusive of substituted acetyl acetone (acac)-containing complexes of vanadium(IV), $VO(acac)_2$, and a bleomycin-vanadium(IV) complex.[39, 40] It was also reported that photocleavage of DNA was achieved using mononuclear vanadium(IV) complexes with red light.[41] In this study, oxidovanadium(IV) complexes [VO(salmet)(B)] and [VO(saltrp)(B)] [where salmet and saltrp are *N*-salicylidene-*L*-methionate and *N*-salicylidene-*L*-tryptophanate, respectively, and B is a N,N-donor heterocyclic base (viz. 1,10-phenanthroline (phen), dipyrido[3,2-d:2',3`-f]quinoxaline (dpq), or dipyrido[3,2-a:2',3`-c]phenazine (dppz))] were found to photocleave DNA.[41] Recently, Chakravarty and co-workers have reported PDT studies involving other vanadium(IV)-containing complexes.[42, 43]

For many years, vanadium(IV) compounds have been reported as insulin-like agents,[44–49] but in the past decade, several vanadium(IV) compounds have also been reported to exhibit anti-cancer activities.[50–54] Previously, bis(4,7-dimethyl-1,10-phenanthroline)sulfatooxovanadium(IV) (metvan) was identified as the most promising multi-targeted anti-cancer compound with apoptosis-inducing activity.[50] Interestingly, in this study, metvan was found to be highly effective against cisplatin-resistant ovarian and testicular cancer cell lines.[50] Following this reasoning, we surmise that a combination of the two metal centres in a single complex may initiate novel properties as PDT agents.

Over the years, our research group has been interested in the synthesis and characterisation of bridging and terminal polypyridyl ligands for the construction of mixed-metal complexes that have at least one ruthenium(II) metal centre. In this work, we have synthesised two novel mixed-metal binuclear complexes containing a ruthenium(II) photosensitiser and a vanadium(IV) metal centre with bridging and terminal polypyridyl-like ligands; then used the two complexes as potential photodynamic therapeutic agents for melanoma cell growth inhibition. Although there was a report of the formation and properties of a stable binuclear mixed-metal complex with ruthenium(II) and vanadium(IV) ($[(NH_3)_5RuVO(H_2O)_n]^{4+}$), there have not been any reports in the literature of any mixed-metal binuclear complexes

containing a ruthenium(II) photosensitiser and a vanadium(IV) metal centre with bridging and terminal polypyridyl-like ligands, or their use as PDT agents.

Results and discussion

Complex **1** was synthesised (Scheme 1) in a reasonable yield by the reaction involving $[Ru(pbt)_2Cl_2]\bullet 0.25CH_3COCH_3$ and $phen_2DTT$; while complex **2** was synthesised (Scheme 1) by reacting 1,10-phenanthroline-5,6-diamine ($phen(NH_2)_2$) with $[Ru(pbt)_2(phendione)](PF_6)_2\bullet 4H_2O$ (where phendione = 1,10-phenanthroline-5,6-dione).

Complex **3** (Scheme 2) was synthesised by reacting [VO(sal-*L*-tryp)(H_2O)] with complex **2**; while complex **4** (Scheme 2) was produced by reacting complex **1** with [VO(sal-*L*-tryp)(H_2O)]. All complexes were characterised by elemental analysis, HRMS, ESI MS, UV-visible absorption, ESR spectroscopy, and cyclic voltammetry, where appropriate.

Figure 1 shows the structures of [VO(sal-*L*-tryp)(H_2O)],[54, 55] [VO(sal-*L*-tryp)(phen)]•H_2O, [VO(sal-*L*-tryp)(MeATSC)]•$1.5C_2H_5OH$ (where MeATSC = 9-anthraldehyde-*N*(4)-methylthiosemicarbazone),[54, 55] [VO(sal-*L*-tryp)(*N*-Ethhymethohcarbthio)]•H_2O (where *N*-ethhymethohcarbthio = (*E*)-*N*-ethyl-2-(4-hydroxy-3-methoxybenzylidene)hydrazinecarbothioamide),[54, 55] [VO(sal-*L*-tryp)(acetylethTSC)]•C_2H_5OH (where acetylethTSC = (*E*)-*N*-ethyl-2-(1-(thiazol-2-yl)ethylidene)hydrazinecarbothioamide),[54, 55] and [Zn(sal-*L*-tryp)(H_2O)]•$0.25H_2O$,[55] which will be discussed in the sections below.

ESI MS analysis

Low resolution ESI MS data were acquired for complexes **1–4**, while HRMS data was acquired for complexes **3** and **4** (see ESI, Fig. S1–S4). In all mass spectral analyses, we have assigned M as the molecular ion minus any solvates. A base peak for complex **1** gave the following m/z value: 1181.08 (100%, $[M - PF_6]^+$); also a peak for $[M - 2PF_6]^{2+}$ was observed at m/z = 518.17.

Complex **2** gave the following m/z value: 1055.00 (100%, $[M - PF_6]^+$); also a peak for $[M - 2PF_6]^{2+}$ was observed at m/z = 455.08. Complex **3** gave the following m/z value: 660.65 (100%, $[M - 2PF_6 + Na - 2H]^+$); also peaks for $[M - PF_6]^+$, $[M - (VO(sal\text{-}L\text{-}tryp)) - PF_6)^+$, $[M - 2PF_6]^{2+}$, and $[M - (VO(sal\text{-}L\text{-}tryp)) - PF_6)^{2+}$ were observed at m/z = 1428.21, m/z = 1055.05, m/z = 641.09, and m/z = 455.01, respectively. On the other hand, complex **4** gave the following m/z value: 1554.00 (100%, $[M - PF_6]^+$); also peaks for $[M - (VO(sal\text{-}L\text{-}tryp)) - PF_6)^+$, $[M - 2PF_6]^{2+}$, and $[M - (VO(sal\text{-}L\text{-}tryp)) - PF_6)^{2+}$ were observed at m/z = 1181.08, m/z = 704.42, and m/z = 517.92, respectively. We believe that the other peaks in the ESI mass spectra of complexes **3** and **4** are due to occurrence of some unidentified species that are formed in the chamber of the mass spectrometer. When HRMS data were acquired, the following peaks were identified where *m/z* = 1428.1035 (100%, $[M - PF_6]^+$) for complex **3**, while for complex **4**, *m/z* = 1554.1096 (100%, $[M - PF_6]^+$).

FT IR and UV-visible spectroscopic studies

Previously, FT IR spectra were acquired for [VO(sal-*L*-tryp)(H_2O)], and [Zn(sal-*L*-tryp)(H_2O)]•0.25H_2O.[55] In this study, FT IR spectra were acquired for [VO(sal-*L*-tryp)(phen)]•H_2O and complexes **3** and **4** (see ESI, Fig S5). Based on the data for the assigned stretching frequencies (see ESI, Table 1), a phenolate ν(C-O) stretching frequency in the region 1551–1538 cm^{-1} is observed for [VO(sal-*L*-tryp)(phen)]•H_2O, [VO(sal-*L*-tryp)(H_2O)],[55] [Zn(sal-*L*-tryp)(H_2O)]•0.25H_2O,[55] complex **3**, and complex **4**. A broad ν(OH) stretching frequency is observed at 3014, 3233, and 3256 cm^{-1} for [VO(sal-*L*-tryp)(H_2O)], [VO(sal-*L*-tryp)(phen)]•H_2O, and [Zn(sal-*L*-tryp)(H_2O)]•0.25H_2O, respectively.[54, 55] The absence of ν(OH) stretching frequencies in compounds **3** and **4** confirms coordination of the Schiff base ligand to the vanadium(IV) metal centre via the phenolate anion.[54, 56, 57]

[VO(sal-*L*-tryp)(H_2O)], [VO(sal-*L*-tryp)(phen)]•H_2O, complex **3**, and complex **4** exhibit ν(V=O) stretching frequencies in the region 956–997 cm^{-1}, which is the typical range for oxidovanadium(IV) complexes.[54, 58, 59]

The UV-visible spectrum of [VO(sal-*L*-tryp)(phen)]•H_2O in DMSO (Figure 2), shows an absorbance at 710 nm, with a molar extinction coefficient of 29 M^{-1} cm^{-1}. This band is due to the d-d transition of the $3d^1$ electronic configuration for the vanadium(IV) metal centre.

All of the ruthenium(II)-containing complexes (Figure 2) have extensive light absorbing properties which are characterised by UV-visible spectroscopy. Complexes **1–4** all possess intense intra-ligand transitions in the UV region, while the lowest Ru(dπ)→bridging ligand (BL) CT bands occur in the low energy visible spectrum. The metal-toligand charge transfer (MLCT) band for complexes **1–3**, occurs at 466 nm; while that for complex **4** occurs at 462 nm. The band (λ = 710 nm, with a very low molar extinction coefficient of 29 M^{-1} cm^{-1}) which is due to the d-d transition of the d^1 electronic configuration for the V(IV) metal centre is not found in our mixed-metal binuclear ruthenium(II)-vanadium(IV) complexes **3** and **4** due to the very highly absorbing feature of the ruthenium(II) metal centre in each complex. The molar extinction coefficients for all complexes are listed in Table 1.

X-band ESR spectroscopic studies

In this study, ESR spectroscopy is used to gather relevant information about the complexes that contain the paramagnetic vanadium(IV) metal centre. As such, we now report X-band ESR spectroscopic studies for [VO(sal-*L*-tryp)(phen)]•H_2O, complex **3**, and complex **4** in DMSO at 10 K, having initially acquired each spectrum at 130 K. Due to the fact that better hyperfine splittings are seen at lower temperatures, we decided to acquire each ESR spectrum at 10 K. The observed hyperfine structure (Figure 3) shows sixteen line ESR signals with partial overlap on three lines. Figure 3 shows three ESR spectra for [VO(sal-*L*-tryp)(phen)]•H_2O, complex **3**, and complex **4** in DMSO, but Figure S6 (see ESI) shows the respective ESR spectra for [VO(sal-*L*-tryp)(phen)]•H_2O, complex **3**, and complex **4** in DMSO along with their simulations. These spectra are characteristic of frozen solution spectra consistent with vanadyl (VO^{2+})-containing complexes, indicating that the freshly prepared vanadium metal centre has a +4 oxidation state for complexes **3** and **4**. The anisotropic sixteen line frozen solution ESR spectra are due to the hyperfine interaction

between the electron spin and the nuclear spin of ^{51}V(IV) (I = 7/2, 100% natural abundance).

The frozen solution ESR spectra of [VO(sal-*L*-tryp)(phen)]•H_2O, complex **3**, and complex **4** were simulated to determine the magnitudes of the principal ^{51}V hyperfine coupling matrix (A_{xx}, A_{xx}, and A_{zz}) and g matrix using the ESR simulation programme XSophe from Bruker BioSpin.

More recently, Lewis *et al*. reported the ESR spectrum for [VO(sal-*L*-tryp)(H_2O)],[54] which was compared with those of complexes **3** and **4**. The ESR parameters (obtained from spectral simulations) for [VO(sal-*L*-tryp)(H_2O)],[54] [VO(sal-*L*-tryp)(phen)]•H_2O, complex **3**, and complex **4** are shown in Table 2. The large A values and broader linewidths are presumably due to the nitrogen ligation and hexacoordination geometry. It must be noted that the ESR spectra of complexes **3** and **4** are similar to those of [V^{IV}O(SAA)(phen)]•H_2O (where SAA = salicylidene anthranilic acid)[60] and [VO(van-tyr)(H_2O)]•0.5EtOH•H_2O (where van-tyr = Schiff base of *o*-vanillin and *L*-tyrosine).[61] This feature and the fact that the spectra and ESR parameters (Table 2) of complexes **3** and **4** are very similar to that of [VO(sal-*L*-tryp)(phen)]•H_2O proves that there is no communication between the ruthenium(II) and vanadium(IV) metal centres.

The ESR spectra of the complexes described here may be useful in future comparison studies of VO^{2+} in complexes and biological systems. Nevertheless, these ESR results are in agreement with those of HRMS, ESI MS, and FT IR spectral measurements, and thus prove that complexes **3** and **4** have a vanadium(IV) metal centre at 10 K. On another note, we plan to carry out future studies involving DFT calculations for [VO(sal-*L*-tryp)(H_2O)], [VO(sal-*L*-tryp)(phen)]•H_2O, complex **3**, and complex **4** in order to elucidate the dependence of calculated ^{51}V A_z values on the orientation and geometry of the respective ligands in these complexes. Such a study involving calculated and experimental A_z values for the respective vanadium(IV)-containing complexes would complement the excellent piece of data for V^{IV}O complexes as reported by Garriba and co-workers.[62–65] Elemental analysis, HRMS, ESI MS, FT IR, and ESR spectroscopic data are consistent with the proposed structures of complexes **1**–**4**.

Electrochemical studies

1. In either acetonitrile or DMSO—Cyclic voltammograms (CVs) of [VO(sal-*L*-tryp)(phen)]•H_2O and complexes **1**–**4** in their respective solvent are shown in Figure 4. Due to the poor solubility of [VO(sal-*L*-tryp)(phen)]•H_2O and complex **4** in CH_3CN, the CVs were recorded in DMSO, where the redox activity in the cathodic region was well-behaved. This behaviour as shown by complex **4** has been shown by complexes containing large aromatic ligands as reported by Richter and Brewer,[66] and by Downard *et al*.[67] In DMSO, it was not possible to observe the redox activity (in the anodic region where the $Ru^{II/III}$ couple is located) for complex **4** due to the limitation of DMSO as a solvent. We did not acquire the CVs for the "free" $phen_2$DTT and tpphz ligands as we were focusing on the redox activity of the metal centre in all complexes in this study. Another reason is the fact that we were unable to obtain the CV for the "free" tpphz ligand due to its poor solubility in either

acetonitrile or DMSO. In such a case, we would not have been able to compare the redox activity of both “free” ligands. Table 3 shows the respective electrochemical data obtained for [VO(sal-*L*-tryp)(H_2O)],[54, 55] [VO(sal-*L*-tryp)(phen)]•H_2O, [VO(sal-*L*-tryp)(MeATSC)]•1.5C_2H_5OH,[54, 55] [VO(sal-*L*-tryp)(*N*-Ethhymethohcarbthio)]•H_2O,[54, 55] [VO(sal-*L*-tryp)(acetylethTSC)]•C_2H_5OH,[54, 55] [Zn(sal-*L*-tryp)(H_2O)]•0.25H_2O,[55] and complexes **1**–**4** in their respective solvent.

Comparison of the CV data for these complexes allows assignation of each redox couple. Due to the fact that the zinc(II) metal centre is known to be redox inactive,[68] electrochemical data acquired for [Zn(sal-*L*-tryp)(H_2O)]•0.25H_2O[55] is used to assign the redox data acquired for all vanadium(IV)-containing complexes in Table 3. Kianfar and Mohebbi[69] reported that the CV acquired for [VO(salen)] exhibited an irreversible anodic redox peak at +0.50 V, which is attributed to the $V^{IV/V}$ redox couple. According to Maia *et al*.,[70] electrochemical data acquired for V(IV) complexes were used to show that irreversible anodic redox couples occurred in the region +0.60 V to +0.65 V, which is attributed to the $V^{IV/V}$ redox couple.[70] Our vanadium(IV)-containing complexes exhibited irreversible $V^{IV/V}$ redox couple in the range +0.14 to +0.22 V.

An irreversible anodic redox peak attributed to the oxidation of the *L*-tryptophan moiety of the Schiff base ligand was observed in the CVs for [VO(sal-*L*-tryp)(H_2O)], [VO(sal-*L*-tryp)(MeATSC)]•1.5C_2H_5OH, [VO(sal-*L*-tryp)(*N*-Ethhymethohcarbthio)]•H_2O, [VO(sal-*L*-tryp)(acetylethTSC)]•C_2H_5OH, [Zn(sal-*L*-tryp)(H_2O)]•0.25H_2O, and complex **3**. The irreversible oxidation of the *L*-tryptophan moiety has been reported to occur at +0.75 V for K[(sal-*L*-tryp)],[55] and at +0.71 V for [Zn(sal-*L*-tryp)(H_2O)]•0.25H_2O.[55]

CVs acquired for oxidovanadium(IV) complexes are also known to display cathodic quasi-reversible voltammetric responses attributed to the V(IV)/V(III) redox couple, in the potential range −0.9 V to −1.3 V.[41]

We were able to assign the reversible couple of $Ru^{II/III}$ for complexes **1**, **2**, and **3**, where $E_{½}$ values occurred at +1.06 V for complex **1**, and at +1.12 V for complexes **2** and **3**.

2. In aqueous media—Preliminary electrochemical studies of the chloride salt of compound **3**, [$Ru(pbt)_2$(tpphz)VO(sal-*L*-tryp)]Cl_2 in pH 7 is presented in Figure 4. It is interesting to note that, in contrast to the CV in organic solvent, only two anodic features are seen, for example, a prefeature at +1.00 V, and a large peak at +1.41 V. Both peaks appear to be irreversible. We tentatively assign these respective peaks to $Ru^{II/III}$ oxidation and a ligand-based oxidation, where the latter assignment is made based on the broad nature of the peak. For comparison, the widely used photosensitser [$Ru(bpy)_3$]Cl_2 gives one reversible redox couple, where the $E_{½}$ value of +1.08 V is assigned to the $Ru^{II/III}$transition. These results suggest a net electron-donating effect of the pbt and tpphz ligands to the ruthenium(II) metal center with respect to [$Ru(bpy)_3$]Cl_2. However, instability of the ligands to high potentials likely prevents the $Ru^{II/III}$ couple in [$Ru(pbt)_2$(tpphz)VO(sal-*L*-tryp)]Cl_2 from being reversible. The cathodic region involving [$Ru(pbt)_2$(tpphz)VO(sal-*L*-tryp)]Cl_2 shows the presence of irreversible and reversible redox couples likely due to $V^{IV/III}$ and ligand-based reductions and oxidations, respectively. We believe that the E_{pc} value of −0.65

V could be ascribed to the $V^{IV/III}$ redox couple,[55] while the $E_{½}$ value of −0.86 V and the E_{pc} value of −1.09 V could be ligand-based. In the future, more detailed electrochemical studies will be carried out on $[Ru(pbt)_2(tpphz)VO(sal\text{-}L\text{-}tryp)]Cl_2$, and $[Ru(pbt)_2(phen_2DTT)VO(sal\text{-}L\text{-}tryp)]Cl_2$ in aqueous media.

Stability studies with $[Ru(pbt)_2(tpphz)VO(sal\text{-}L\text{-}tryp)]Cl_2$ and $[Ru(pbt)_2(phen_2DTT)VO(sal\text{-}L\text{-}tryp)]Cl_2$ in aqueous media

Stability studies with $[Ru(pbt)_2(tpphz)VO(sal\text{-}L\text{-}tryp)]Cl_2$, and $[Ru(pbt)_2(phen_2DTT)VO(sal\text{-}L\text{-}tryp)]Cl_2$ in aqueous media were performed at pH 7.19. Such studies were carried out by using ESR and ^{51}V NMR spectroscopic techniques to ascertain whether there was any oxidation of the vanadium(IV) metal centre to a vanadium(V) metal centre in the presence of air, or whether there was formation of any other vanadium(V) species should there be degradation of $[Ru(pbt)_2(tpphz)VO(sal\text{-}L\text{-}tryp)]Cl_2$, and $[Ru(pbt)_2(phen_2DTT)VO(sal\text{-}L\text{-}tryp)]Cl_2$ in aqueous media. As such, ^{51}V NMR spectroscopy was used as a complement to ESR spectroscopy should there be any degradation of the complexes and formation of vanadate oligomers. If this were to happen, we should observe the following chemical shifts for the respective species: mononuclear V_1 ($\delta = -559$ ppm), dinuclear V_2 ($\delta = -572$ ppm), tetranuclear V_4 ($\delta = -576$ ppm), and pentanuclear V_5 ($\delta = -584$ ppm).[71, 72] In our study, we acquired ESR and ^{51}V NMR spectra of 4.0 mM aqueous solutions of $[Ru(pbt)_2(tpphz)VO(sal\text{-}L\text{-}tryp)]Cl_2$, and $[Ru(pbt)_2(phen_2DTT)VO(sal\text{-}L\text{-}tryp)]Cl_2$ (pH 7.19) at 0, 24, 48, and 72 hours at room temperature. It must be stressed that a ^{51}V NMR spectrum was also acquired for a 4.0 mM solution of $NaVO_3$ (pH 7.19) as a control. We also acquired ^{51}V NMR spectra for the solutions seven days later.

Figure 5 shows the respective spectra as acquired for 4.0 mM $VOSO_4$ in 0.1 M H_2SO_4, $[Ru(pbt)_2(tpphz)VO(sal\text{-}L\text{-}tryp)]Cl_2$, and $[Ru(pbt)_2(phen_2DTT)VO(sal\text{-}L\text{-}tryp)]Cl_2$. In Figure 5A, it can be seen that both complexes possess complicated ESR spectra in aqueous media. The isotropic (motionally averaged) ESR spectrum that is observed for $VOSO_4$ (see Figure 5)[73] is not observed for $[Ru(pbt)_2(tpphz)VO(sal\text{-}L\text{-}tryp)]Cl_2$, and $[Ru(pbt)_2(phen_2DTT)VO(sal\text{-}L\text{-}tryp)]Cl_2$. The spectra resemble spectra that are produced from the binding of the small vanadyl cation to large proteins, where highly anisotropic (slow motion averaged) spectra are observed.[73, 74] As such this feature could be due to the presence of the large nuclei of V and Ru which may cause an anisotropic tumble with a very slow tumbling rate perpendicular to the inter-nuclear vector. It must be noted that there is no decrease in intensity for the ESR spectra at 0, 24, 48, and 72 hours. On the other hand, with the use of ^{51}V NMR spectroscopy, the data in Figure 5B shows the absence of any vanadium(V) species up to 72 hours, but on day seven, a weak, broad peak at −543 ppm which is due to the presence of a vanadium(V) species was observed for both complexes. The structure of this vanadium(V) species has not been determined, but clearly, it is not any of the vanadate oligomers (see Figure 5B for the ^{51}V NMR spectrum of $NaVO_3$).[71, 72]

In summary, both ESR and ^{51}V NMR spectroscopic studies proved that on standing at room temperature, there is considerable stability of $[Ru(pbt)_2(tpphz)VO(sal\text{-}L\text{-}tryp)]Cl_2$, and $[Ru(pbt)_2(phen_2DTT)VO(sal\text{-}L\text{-}tryp)]Cl_2$, where the vanadium(IV) metal centre appears to

be resistant to oxidation in aqueous media. This chemical property is similar to that of [VIVO(LASSBio1064-2H)(phen)]•H_2O (where LASSBio1064 = (*E*)-N'-(2-hydroxybenzylidene-4-chlorobenzohydrazide) as reported by Benítez *et al*.[75]

Biological studies

After fully characterising complexes **3** and **4**, dark and light toxicity studies were conducted with their chloride salts. Such studies were carried out on A431, human epidermoid carcinoma cells; amelanotic malignant melanoma cells; and non-cancerous HFF, human skin fibroblast cells. In some cases, $Na_4[Co(tspc)(H_2O)_2]$ and [VO(sal-*L*-tryp)(phen)]•H_2O were also used in these studies. The choice of using $Na_4[Co(tspc)(H_2O)_2]$ is based on the fact that many photoactive species have been synthesised in a similar fashion to porphyrins and chlorins, and the fact that phthalocyanines show a strong light absorption at wavelengths around 670 nm (see ESI, Fig. S7 for the UV-visible spectrum of $Na_4[Co(tspc)(H_2O)_2]$ in water) and are therefore well-adapted to the optical window required for PDT application. The choice of $Na_4[Co(tspc)(H_2O)_2]$ is warranted based on the fact that we wish to assess the PDT nature of this complex before carrying out any PDT studies with the "free" base (H_2) of a phthalocyanine (Pc) dye, copper (Cu), copper di-, tri-, tetra-sulfonated (CuS_2, CuS_3, CuS_4), fluoro chromium (FCr), iron (Fe), palladium tetra-sulfonated (PdS_4), nickel (Ni), and nickel tetra-sulfonated (NiS_4)Pc dyes as reported by Chan *et al*.,[76] or other phthalocyanine-containing complexes as reported by other researchers.[77–79] It must be stressed that a PDT study which involved $Na_4[Co(tspc)(H_2O)_2]$ was reported by Chan *et al*,[76] where the cobalt(II) complex had no cytotoxic activity in assays with murine embryonic fibroblasts or fibrosarcoma cells under conditions of either room-light or red-light exposure. We still decided to use $Na_4[Co(tspc)(H_2O)_2]$ in our PDT studies as this complex may have some form of anti-cancer properties against the selected cell lines.

Due to the fact that [VO(sal-*L*-tryp)(phen)]•H_2O was used in the photocleavage of DNA with red light,[41] we thought that it would have been appropriate to use such a complex in our dark toxicity study; followed by later work to assess its viability as a PDT agent after carrying out light toxicity studies. In the light toxicity studies, we utilised the synergistic effect of the *L*-tryptophan-containing Schiff base (as it has been observed that the *L*-tryptophan compound with a photoactive indole ring shows a significantly enhanced DNA photocleavage activity when compared to its *L*-phenylalanine analogue[80–82]) and the presence of ruthenium(II) and vanadium(IV) metal centers as effective PDT agents that can absorb in the NIR while possessing very large molar extinction coefficients of ~ 1000 M^{-1} cm^{-1} or higher. Also, complexes **3** and **4** have intense, overlapping MLCT transitions in the visible region of the spectrum for acceptor ligand and ligand-based $\pi \rightarrow \pi^*$ transitions in the UV region. From Figure 2, we found that complex **3** absorbs very weakly at wavelengths > 600 nm, but complex **4** possesses a greater absorption in the red and NIR regions as determined from the following molar extinction coefficients: ε_{630} = 192 M^{-1} cm^{-1}, ε_{740} = 101 M^{-1} cm^{-1}, and ε_{800} = 111 M^{-1} cm^{-1}, all which can be compared to ε_{630} = 3500 M^{-1} cm^{-1} for Photofrin.[37] It is also expected that these complexes can efficiently absorb light throughout the UV and visible regions, thus allowing for efficient excitation. The MLCT emissions of these complexes are expected to be quenched by oxygen to produce $^1O_2$.[83]

(A) Dark toxicity with [VO(sal-*L*-tryp)(phen)]•H_2O, $Na_4[Co(tspc)(H_2O)_2]$, $[Ru(pbt)_2(tpphz)VO(sal\text{-}L\text{-}tryp)]Cl_2$, and $[Ru(pbt)_2(phen_2DTT)VO(sal\text{-}L\text{-}tryp)]Cl_2$ in the presence of A431, human epidermoid carcinoma cells and HFF, human skin fibroblast cells—The objective of this study is to evaluate the anti-proliferative activity of [VO(sal-*L*-tryp)(phen)]•H_2O, $Na_4[Co(tspc)(H_2O)_2]$, $[Ru(pbt)_2(tpphz)VO(sal\text{-}L\text{-}tryp)]Cl_2$, and $[Ru(pbt)_2(phen_2DTT)VO(sal\text{-}L\text{-}tryp)]Cl_2$ against A431 carcinoma cells, and to compare their anti-proliferative activity on non-cancerous HFF cells. [VO(sal-*L*-tryp)(phen)]•H_2O, $Na_4[Co(tspc)(H_2O)_2]$, $[Ru(pbt)_2(tpphz)VO(sal\text{-}L\text{-}tryp)]Cl_2$, $[Ru(pbt)_2(phen_2DTT)VO(sal\text{-}L\text{-}tryp)]Cl_2$, and cisplatin were evaluated for their cytotoxicity on these cell lines by means of using the 3-(4,5-dimethylthiazol-2-yl)-2,5-diphenyltetrazolium bromide (MTT) colorimetric assay.[84] The effects of the compounds on the viability of these cells were evaluated after incubation for 24 hours. We were able to discern differences in the degrees of toxicity between each compound examined (Figure 6 and ESI, Fig. S8) with the two cell lines.

The results demonstrated the greatest difference in the inhibition of cell proliferation between cancerous A431 and non-cancerous HFF cells. [VO(sal-*L*-tryp)(phen)]•H_2O and $[Ru(pbt)_2(tpphz)VO(sal\text{-}L\text{-}tryp)]Cl_2$ were found to be the most active of the four complexes tested; followed by $[Ru(pbt)_2(phen_2DTT)VO(sal\text{-}L\text{-}tryp)]Cl_2$. In this study, [VO(sal-*L*-tryp)(phen)]•H_2O, $[Ru(pbt)_2(tpphz)VO(sal\text{-}L\text{-}tryp)]Cl_2$, and $[Ru(pbt)_2(phen_2DTT)VO(sal\text{-}L\text{-}tryp)]Cl_2$ were shown to decrease the cell viability of A431 carcinoma cells (Table 4), where the IC_{50} values were 41.615 ± 5.8, 41.25 ± 7.6, and 48.6 ± 13.1 μM, respectively. $Na_4[Co(tspc)(H_2O)_2]$ was found to be non-toxic to either cancerous A431 cells (the IC_{50} value was greater than 1000 but less than 2000 μM) or the non-cancerous HFF cells (IC_{50} value >2000 μM. $[Ru(pbt)_2(tpphz)VO(sal\text{-}L\text{-}tryp)]Cl_2$ and $[Ru(pbt)_2(phen_2DTT)VO(sal\text{-}L\text{-}tryp)]Cl_2$ were found to be less toxic to the non-cancerous HFF cells (IC_{50} values = 100.7 ± 17.7 and 204.4 ± 45.1 μM, respectively) when compared to the higher toxicity of [VO(sal-*L*-tryp)(phen)]•H_2O (IC_{50} value = 63.1 ± 28.3 μM). When compared to the standard, cisplatin in this dark toxicity study, all complexes with the exception of $Na_4[Co(tspc)(H_2O)_2]$, were found to be similarly toxic to the A431, human epidermoid carcinoma cells (see Table 4). The IC_{50} values of [VO(sal-*L*-tryp)(phen)]•H_2O, $[Ru(pbt)_2(tpphz)VO(sal\text{-}L\text{-}tryp)]Cl_2$ and $[Ru(pbt)_2(phen_2DTT)VO(sal\text{-}L\text{-}tryp)]Cl_2$ were comparable to the IC_{50} value of cisplatin.

(B) Light toxicity of $[Ru(pbt)_2(tpphz)VO(sal\text{-}L\text{-}tryp)]Cl_2$ and $[Ru(pbt)_2(phen_2DTT)VO(sal\text{-}L\text{-}tryp)]Cl_2$ with a 740 nm LED lamp in A431 and HFF cells—As there is a desire to use PDT agents within the “phototherapeutic window” of 620–850 nm, we decided to test $[Ru(pbt)_2(tpphz)VO(sal\text{-}L\text{-}tryp)]Cl_2$ and $[Ru(pbt)_2(phen_2DTT)VO(sal\text{-}L\text{-}tryp)]Cl_2$ as new PDT agents for A431 cell growth inhibition with red light (peak wavelength range 715–745 nm, maximum at 740 nm). Since [VO(sal-*L*-tryp)(phen)]•H_2O absorbs NIR light at 710 nm, we expect $[Ru(pbt)_2(tpphz)VO(sal\text{-}L\text{-}tryp)]Cl_2$ and $[Ru(pbt)_2(phen_2DTT)VO(sal\text{-}L\text{-}tryp)]Cl_2$ to absorb NIR light at 710 nm (due to the presence of the vanadium(IV) metal centre), which is within the “phototherapeutic window” of 620–850 nm., We tested the *in vitro* efficacy of $[Ru(pbt)_2(tpphz)VO(sal\text{-}L\text{-}tryp)]Cl_2$ and $[Ru(pbt)_2(phen_2DTT)VO(sal\text{-}L\text{-}tryp)]Cl_2$ because of their cytopathic effect on A431, as determined by IC_{50} values in our dark studies (Table

4). To test whether light exposure further enhance the efficacy of these metal complex toward cancer cells, we compared light toxicity results with additional dark studies carried out for both compound-cell combinations under identical experimental conditions.

We detected no cell death under both dark and light exposure at 0 μM while only minor changes in morphology occurred at 5 μM and 20 μM in our non cancerous HFF cells. Although only slight changes in cell morphology were observed at 5 μM, both compounds showed their anticancer cytopathic effect on A431 cells at 20 μM (Figures 7A through D). When compared to respective dark toxicity results, both $[Ru(pbt)_2(tpphz)VO(sal\text{-}L\text{-}tryp)]Cl_2$ and $[Ru(pbt)_2(phen_2DTT)VO(sal\text{-}L\text{-}tryp)]Cl_2$ showed light enhanced cytopathic effects in A431 carcinoma cells in contrast to no effect observed in our control skin fibroblast cells (Figures 7A through D). We also observed more pronounced light enhancement of cancer cell death in presence of $[Ru(pbt)_2(phen_2DTT)VO(sal\text{-}L\text{-}tryp)]Cl_2$ when compared to $[Ru(pbt)_2(tpphz)VO(sal\text{-}L\text{-}tryp)]Cl_2$ treated cells (Figures 7B and 7D).

(C) Dark and light toxicity of $Na_4[Co(tspc)(H_2O)_2]$ and $[Ru(pbt)_2(tpphz)VO(sal\text{-}L\text{-}tryp)]Cl_2$ with a 60 W tungsten lamp in the presence of amelanotic malignant melanoma cells—Dark and light toxicity studies on amelanotic malignant melanoma cells were performed to further test whether this cancer cell line is sensitive to $[Ru(pbt)_2(tpphz)VO(sal\text{-}L\text{-}tryp)]Cl_2$ or $Na_4[Co(tspc)(H_2O)_2]$ (where in water, $\varepsilon_{740} = 4.2 \times 10^3\ M^{-1}\ cm^{-1}$). Amelanotic malignant melanoma cells were placed in well plates, and once the cells were confluent designated wells were treated with $Na_4[Co(tspc)(H_2O)_2]$ or $[Ru(pbt)_2(tpphz)VO(sal\text{-}L\text{-}tryp)]Cl_2$ at concentrations of 5.0 and 20.0 μM. As a control, the melanoma cells were cultured in the absence of $Na_4[Co(tspc)(H_2O)_2]$ and $[Ru(pbt)_2(tpphz)VO(sal\text{-}L\text{-}tryp)]Cl_2$ (Figure 8A–B). To determine the dark toxicity of $Na_4[Co(tspc)(H_2O)_2]$ and $[Ru(pbt)_2(tpphz)VO(sal\text{-}L\text{-}tryp)]Cl_2$, the cells were incubated with the complexes for one day in the dark. At concentrations of 5.0 and 20.0 μM of $Na_4[Co(tspc)(H_2O)_2]$ (incubated in the dark), the melanoma cells do not show significant apoptosis (Figure 8A, upper panel). Cell studies involving $[Ru(pbt)_2(tpphz)VO(sal\text{-}L\text{-}tryp)]Cl_2$ on the other hand show some morphological changes of the melanoma cells at 20.0 μM (Figure 8B, upper panel) when incubated in the dark.

The light experiments were carried out on melanoma cells in the presence and absence of $Na_4[Co(tspc)(H_2O)_2]$ and $[Ru(pbt)_2(tpphz)VO(sal\text{-}L\text{-}tryp)]Cl_2$. The cells were placed in well plates, and once the cells were confluent, designated wells were treated with $Na_4[Co(tspc)(H_2O)_2]$ and $[Ru(pbt)_2(tpphz)VO(sal\text{-}L\text{-}tryp)]Cl_2$ at 5 and 20 μM as before. After 24 hours of incubation following treatment, the cells were irradiated with a 60 W tungsten lamp for 30 minutes; then incubated for three hours before phase contrast photos were taken (Figure 8A–B, lower panel). Minor apoptosis occurred when the melanoma cells were irradiated in the presence of $[Ru(pbt)_2(tpphz)VO(sal\text{-}L\text{-}tryp)]Cl_2$ at 5 μM, but the melanoma cells show complete apoptosis when irradiated at 20 μM (Figure 8B, lower panel). On the other hand, $Na_4[Co(tspc)(H_2O)_2]$ had no impact on the melanoma cells at either 5 or 20 μM under illumination (Figure 8A, lower panal).

Controls in the absence of both $Na_4[Co(tspc)(H_2O)_2]$ and $[Ru(pbt)_2(tpphz)VO(sal\text{-}L\text{-}tryp)]Cl_2$, with or without irradiation, resulted in no cell death, similar to the results reported by Hong and co-workers.[35]

Our findings have potential significance for the clinical use of our complexes (with Schiff bases of *L*-tryptophan), for example, the chloride salts of complexes **3** and **4** in PDT. Interestingly, the serum *L*-tryptophan level of some cancer patients (including breast, lung, malignant melanoma, and ovarian) is depleted relative to normal controls.[85, 86] This is thought to be due to the activity of indoleamine 2,3-dioxygenase, which converts it to kynuren-ine.[85, 86] It is possible that if *L*-tryptophan is depleted in cancer patients, and if this is a general finding, then such depletion may aid the effectiveness of the chloride salts of complexes **3** and **4** in PDT.

In the future, we also plan to carry out an extensive photochemical studies on complexes **1**–**4** in order to determine the various life-times, quantum yields, and fluorescence properties in acetonitrile and aqueous media.

It is also imperative to carry out *in vitro* studies to determine the IC_{50} values in the dark and in the presence of light at various wavelengths, for example, 470, 630, and 740 nm, for complexes **1–4** as chloride salts and $Na_4[Co(tspc)(H_2O)_2]$. Also, Photofrin and cisplatin will be used as controls in these studies. Light studies will prove whether the presence of the L-tryptophan and polypyridyl moieties with ruthenium(II) and vanadium(IV) metal centres all in one complex do facilitate synergistic effects necessary for PDT within the PDT spectral window of 600–800 nm. After these studies, ESR and ^{51}V NMR spectroscopy will be used in order to determine whether any vanadium(IV)- or vanadium(V)-containing species are formed after the irradiation process. Side effects of chemotherapeutic drugs are not just additional burdens to cancer patients but real problems during the treatments. Also, it must be stated that the lack of selective accumulation of these photo-activable complexes within tumour tissue is a major problem in PDT, thus we will have to develop targeted photosensitisers. Targeted photodynamic therapy can enhance photodynamic efficiency by directly targeting diseased cells or tissues. We must identify ways to either increase the uptake of the complexes by the target cells and tissues or to improve subcellular localisation so as to deliver the complexes to photosensitive sites within the cells. Various drug delivery strategies employing nano-technologies (liposomes, polymers, quantum dots, dendrimers, etc.) must be developed and innovative targeting methods will have to be established for passive and active targeting. Another key factor for successful site-specific drug delivery is how to control the release of drug from such delivery vehicles in order to achieve higher selectivity toward cancer cells/tumour tissue over surrounding non-cancerous cells/tissues.

Conclusions

We have successfully synthesised novel mixed-metal ruthenium(II)-vanadium(IV) complexes. Results from HRMS, ESI MS, FT IR, and ESR spectroscopic characterisation proved that mixed-metal binuclear ruthenium(II)-vanadium(IV) complexes (**3** and **4**) had the predicted structures. From data acquired from *in vitro* studies either in the dark or after irradiation with a 60 W tungsten lamp or a 740 nm LED lamp,

$[Ru(pbt)_2(phen_2DTT)VO(sal\text{-}L\text{-}tryp)]Cl_2$ and $[Ru(pbt)_2(tpphz)VO(sal\text{-}L\text{-}tryp)]Cl_2$ were found to have excellent efficacy in inhibiting melanoma cell growth when compared to $Na_4[Co(tspc)(H_2O)_2]$ in the presence of light as determined in a qualitative study.

Experimental

Materials and methods

Analytical or reagent grade chemicals were used throughout this study. All the chemicals including solvents were obtained from Sigma-Aldrich (St. Louis, MO, USA) or other commercial vendors and used as received. Microanalyses (C, H, N) were performed by CHN and ICP-OES analysis by the Microanalysis Laboratory at the University of Illinois Urbana-Champaign. Also microanalyses (C, H, N, P, and S) were carried out by Galbraith Laboratories, Inc.

ESR spectra were acquired on a Bruker BioSpin EMX^{micro} X-band ESR spectrometer and a Bruker BioSpin Elexsys E500 ESR spectrometer. FT IR spectra were acquired in the range 4000–400 cm^{-1} using the ATR accessory (with a diamond crystal) on a Nicolet 6700 FT IR spectrophotometer. ^{51}V NMR spectra were acquired on a Varian 500 MHz spectrometer with DMSO-d_6 as solvent and $VOCl_3$ as an external reference as described for vanadium(V) compounds.[71]

Electrochemical studies)—Cyclic voltammetric (CV) data were acquired on a Bioanalytical Systems Inc. Epsilon workstation on a C3 cell stand at RT. Either acetonitrile or DMSO solutions which contained 1.0 mM of each analyte and 0.10 M tetra-*n*-butylammonium hexafluorophosphate (TBAP) as supporting electrolyte, were saturated with argon for 15 minutes prior to each acquisition. A blanket of argon gas was maintained throughout the measurements. The measurements were carried out with a three-electrode system consisting of a platinum working electrode, a platinum wire auxiliary electrode, and a Ag/Ag^+ (0.01 M $AgNO_3$ and 0.10 M TBAP in acetonitrile) reference electrode. The working electrode was polished before each experiment with alumina slurry.

Electrochemical studies with $[Ru(pbt)_2(tpphz)VO(sal\text{-}L\text{-}tryp)]Cl_2$ in aqueous media—Cyclic voltammetric studies were acquired on a CH Instruments Electrochemical Workstation using a glassy carbon working electrode, Pt mesh counter electrode, and a Ag/AgCl reference. All solutions of 0.32 mM $[Ru(pbt)_2(tpphz)VO(sal\text{-}L\text{-}tryp)]Cl_2$ with 0.10 M Na_2SO_4 as supporting electrolyte (pH 7) were made up with 2% (v/v) DMSO. Each solution was degassed with nitrogen for 10 minutes prior to acquiring any cyclic voltammograms. The scan rate was 100 mV s^{-1}. Aqueous CV data remained consistent regardless of the direction of the initial scan (positive or negative).

Electronic spectra were recorded using quartz cuvettes on a HP8452 diode array spectrophotometer using acetonitrile, DMSO, or 2:1 MeOH/MeCN (v/v), where appropriate. Each ESI MS was acquired on an HP Agilent 1956b single-quadrupole mass spectrometer. Samples were dissolved in CH_3CN and introduced by direct injection using a syringe pump and a flow rate of 100 μL s^{-1}, while sweeping the cone voltage from 0 to 200 V at a rate of 10 V min^{-1}. HRMS were acquired on a Waters Q-tof Ultima mass spectrometer with a cone

voltage of 25 V. The samples were dissolved in the CH_3CN at 1 mg ml^{-1}; then the resulting solution was diluted with CH_3CN to about 5 ng uL^{-1}. The mobile phase was acetontrile with a flow rate of 50 uL min^{-1}.

Stability studies with $[Ru(pbt)_2(tpphz)VO(sal\text{-}L\text{-}tryp)]Cl_2$, and $[Ru(pbt)_2(phen_2DTT)VO(sal\text{-}L\text{-}tryp)]Cl_2$ in aqueous media—For ESR studies, a 50 mM concentration for each complex was made up with DMSO; then 80 μL of each stock 50 mM solution was added to 920 μL of the DI water (pH 7.19) in order to make diluted solutions of 4.0 mM for ESR measurements. The ESR spectra of the diluted solutions were acquired at room temperature immediately, then at 24, 48, and 72 hours after leaving each solution in subdued light at room temperature.

For ^{51}V NMR studies, ^{51}V NMR spectra were acquired for the 4.0 mM solutions at 0, 24, 48, 72 hours, and seven days later. A control ^{51}V NMR spectrum was also acquired for a 4.0 mM solution of $NaVO_3$ (pH 7.19).

Biological protocols

(A) Dark toxicity with $[VO(sal\text{-}L\text{-}tryp)(phen)]\cdot H_2O$, $Na_4[Co(tspc)(H_2O)_2]$, $[Ru(pbt)_2(tpphz)VO(sal\text{-}L\text{-}tryp)]Cl_2$, and $[Ru(pbt)_2(phen_2DTT)VO(sal\text{-}L\text{-}tryp)]Cl_2$ in the presence of A431, human epidermoid carcinoma cells and HFF, human skin fibroblast cells: The representative cell lines used in the experiments were A431 carcinoma cells and non-cancerous HFF cells. Both cell lines were obtained from the American Type Culture Collection (ATCC). The cells were cultured at 37 °C in high glucose Dulbecco's Modified Eagle Medium (DMEM, Gibco 11965) containing 10% fetal bovine serum and 0.5% penicillin streptomycin (Gibco, 35050).

100 mM stock solutions of $[VO(sal\text{-}L\text{-}tryp)(phen)]\cdot H_2O$, $[Ru(pbt)_2(tpphz)VO(sal\text{-}L\text{-}tryp)]Cl_2$, and $[Ru(pbt)_2(phen_2DTT)VO(sal\text{-}L\text{-}tryp)]Cl_2$ were prepared in DMSO; then the final DMSO concentration in all media was adjusted to 1%. For $Na_4[Co(tspc)(H_2O)_2]$, a 20 mM stock solution was prepared with water as a solvent. Cell viability/growth was measured using the 3-(4,5-dimethylthiazol-2-yl)-2,5-diphenyltetrazolium bromide (MTT) colorimetric assay according to the manufacturer's instructions (Roche Diagnostics, Nutley, NJ).[84] Briefly, the cells were seeded in 96-well tissue culture plates at a density of 1×10^4 cells per well and allowed to adhere overnight. The following day, cells were treated with each complex at concentrations ranging from 1 to 1000 μM for up to 24 hours.

All plates were incubated in dark conditions for 24 hours at 37 °C. After 24 hours, phase contrast images were taken of all cells at 10x magnification using an Olympus IX51 microscope. At the designated time, 10 μl of MTT reagent I was added to the culture media and the plate returned to the 37 °C incubator for four hours, at which time, 100 μl of the solubilization solution (MTT reagent II) was added and incubation continued overnight. Cellular proliferation was determined spectrophotometrically using an enzyme-linked immunosorbent assay (ELISA) plate reader at 590 nm. The MTT assay was validated in our system by the direct trypan blue method.

Also, a 20 mM stock solution of $Na_4[Co(tspc)(H_2O)_2]$ was made with water as a solvent. A 50 mM stock solution of [VO(sal-*L*-tryp)(phen)]•H_2O was made with DMSO as a solvent. Two 40 mM stock solutions of $[Ru(pbt)_2(phen_2DTT)VO(sal\text{-}L\text{-}tryp)]Cl_2$ and $[Ru(pbt)_2(tpphz)VO(sal\text{-}L\text{-}tryp)]Cl_2$ were made with DMSO as a solvent. Cells were seeded into six (6) well plates at a density of 10^5 cells and 2 ml DMEM per well. After 24 hours, the media was replaced with the media containing the appropriate complex at concentrations of 0, 5, and 20 μM. All plates were incubated in dark conditions for 24 hours at 37 °C. After 24 hours, phase contrast images were taken of all cells at 10x magnification using an Olympus IX51 microscope.

(B) Light toxicity of $[Ru(pbt)_2(tpphz)VO(sal\text{-}L\text{-}tryp)]Cl_2$ and $[Ru(pbt)_2(phen_2DTT)VO(sal\text{-}L\text{-}tryp)]Cl_2$ with a 740 nm LED lamp in A431 and HFF cells: The representative cancer cells and control cells used in the experiments were maintained as described in previous section (Section A, Biological protocols).

We prepared a 40 mM stock solution of each complex in DMSO, which was further diluted to 0.10 mM in water. From the 0.1 mM stock, media containing the appropriate compound at concentrations of 0.0, 5.0, and 20.0 μM were prepared in the respective culture media. The final concentration of DMSO in media containing metal complex or controls was maintained at 0.05%. For toxicity studies, representative cells were seeded into six well plates at a density of 8×10^5 cells with 2 ml of respective culture media 24 hours before the treatment with the complex. On the following day, the growth medium was removed and the cells in each well were exposed to 2 ml of the respective medium containing complexes at concentrations of 0.0, 5.0, or 20.0 μM. Separate plates were prepared for light toxicity and dark toxicity studies. Complex treated plates were further incubated under dark conditions at 37 °C for 24 hours with 5% CO_2.

For light toxicity, the cells were exposed for 60 minutes to 740 nm red light (peak wavelength range 715 to 745 nm; minimum output irradiance >560 mW cm^2; active area 4 × 5 cm^2; and light power > 11,250 mW), using a JL3-740F-90 LED (Clearstone Technologies, Inc.), followed by further incubation for 24 hours in the dark. After 24 hours incubation, phase contrast images for both the complex treated cells exposed to light (light toxicity) and control cells incubated in the dark (dark toxicity) were acquired on a Zeiss LSM510 META confocal imaging system (Carl Zeiss Microscopy, LLC Thornwood, NY) at 10× magnification and processed using LSM image browser software.

(C) Dark and light toxicity of $Na_4[Co(tspc)(H_2O)_2]$ and $[Ru(pbt)_2(tpphz)VO(sal\text{-}L\text{-}tryp)]Cl_2$ with a 60 W tungsten lamp in the presence of amelanotic malignant melanoma cells: The representative cancer cells used in the experiments were amelanotic malignant melanoma cells. The cell line was obtained from the American Type Culture Collection (ATCC). The cell line is tumourigenic and was obtained from a 53 year old Caucasian male. The melanoma cells were cultured at 37 °C and 5% CO_2 in high glucose Dulbecco's Modified Eagle Medium (DMEM, Gibco 11965) containing 10% fetal bovine serum, 0.5% penicillin streptomycin (Gibco 15140), 1% glutamine (Gibco 35050) and 1% non-essential amino acids (Gibco 11140). Cells were passaged using 0.25% trypsin (Gibco 25200).

A 100 mM solution of $Na_4[Co(tspc)(H_2O)_2]$ was made with water as solvent, and a 100 mM solution of $Ru(pbt)_2(tpphz)VO(sal\text{-}L\text{-}tryp)]Cl_2$ was made with DMSO as solvent. Before exposure to $Na_4[Co(tspc)(H_2O)_2]$ and $Ru(pbt)_2(tpphz)VO(sal\text{-}L\text{-}tryp)]Cl_2$ at the appropriate concentrations of 5 and 20 μ-M, the cells were seeded into a 6-well plate at a density of 10^5 cells per well. After 24 hours, the media were replaced with media containing the compounds and were incubated 24 hours at 37 °C and 5% CO_2. Following a 24 hour incubation in media containing the metal complexes, the cells were irradiated with a 60 W Tungsten lamp for 30 minute or kept in the dark as controls. The phase contrast images were obtained with an inverted microscope (Nikon TS100) at a magnification of 10x three hours after the light treatment; then processed using MetaMorph imaging software.

Synthesis of ligands and complexes

Ligands—1,4-bis(1,10-phenanthrolin-5-ylsulfanyl)butane-2,3-diol ($phen_2DTT$) was synthesised as reported by Dotsenko *et al.*,[87] while 1,10-phenanthroline-5,6-diamine ($phen(NH_2)_2$) was synthesised as described by Bolger *et al.*[88]

Synthesis of the complexes—$[VO(sal\text{-}L\text{-}tryp)(H_2O)]$ was synthesised using the procedure given by Lewis *et al.*;[54] while $[VO(sal\text{-}L\text{-}tryp)(phen)]\cdot H_2O$ was synthesised following the procedure of Sasmal *et al.*[41] $[Ru(pbt)_2(phendione)](PF_6)_2\cdot 4H_2O$ (where pbt = 2-(2'-pyridyl)benzothiazole) and $[Ru(pbt)_2Cl_2]\cdot 0.25CH_3COCH_3$ were synthesised as described by Cropek *et al.*[89] $Na_4[Co(tspc)(H_2O)_2]$ (where tspc = 4,4',4”, 4”'tetrasulfophthalocyanine) was synthesised according to the method of Weber and Busch.[90]

Synthesis of $[Ru(pbt)_2(phen_2DTT)](PF_6)_2\cdot 1.5H_2O$ 1—1,4-Bis(1,10-phenanthrolin-5-ylsulfanyl)butane-2,3-diol ($phen_2DTT$) (1.27 g, 2.49 mmol) was added to a 500 ml round bottom flask followed by ethylene glycol (25 ml) and 2:1 EtOH:H_2O (400 ml). The mixture was refluxed with stirring until the solid was dissolved completely; then the flask and its contents were removed from the heat; then $[Ru(pbt)_2Cl_2]\cdot 0.25CH_3COCH_3$ (0.76 g, 1.24 mmol) was slowly added to the solution. The reaction mixture was refluxed for 72 hours; then the solution was cooled to room temperature, and finally the mixture was rotary evaporated to remove ethanol from the reaction mixture. NH_4PF_6 (6.0 g, 36.8 mmol) and filtered saturated aqueous KPF_6 (400 ml) was then added to the resulting mixture to precipitate the crude product. The mixture was filtered; then the collected precipitate was air dried. The dried residue was then dissolved in the minimum volume of 2:1 EtOH:MeCN (v/v). The resulting solution was filtered, and the filtrate collected.

The filtrate was loaded onto a Sephadex LH-20 column; then elution was carried out with 2:1 EtOH:MeCN (v/v) as eluent. The fractions with the pure product (as determined by ESI MS analysis) were rotary evaporated to dryness. Yield of product = 1.43 g (85%).

Calc. for $C_{52}H_{41}F_{12}N_8O_{3.5}P_2RuS_4$, C, 46.15; H, 3.05; N, 8.28; P, 4.58; S, 9.48. Found: C, 46.16; H, 2.90; N, 7.84; P, 4.28; S, 8.98. *m/z* (ESI, positive mode): 1181.08 (100%, $[M - PF_6]^+$). UV-visible spectrum (CH_3CN), $\lambda_{max.}$/nm (10^{-4} ε/M^{-1} cm^{-1}): 228 (11), 272 (7.8), 320 (5.5), 344 sh (4.2), and 466 (1.8).

Synthesis of [Ru(pbt)$_2$(tpphz)](PF$_6$)$_2$•3H$_2$O 2—1,10-Phenanthroline-5,6-diamine (phen(NH$_2$)$_2$), 0.87 g, 4.14 mmol) was dissolved in hot methanol (440 mL). [Ru(pbt)$_2$(phendione)](PF$_6$)$_2$•4H$_2$O (2.35 g, 2.14 mmol) was dissolved in acetonitrile (MeCN) (100 ml) in a one (1) litre round bottom flask; then the resulting mixture was refluxed at 80 °C until the solid was dissolved. The previously prepared phen(NH$_2$)$_2$ solution was carefully added down the reflux condenser. This mixture was refluxed for 24 hours at 80 °C. After cooling to room temperature, the mixture was rotary evaporated to dryness; then NH$_4$PF$_6$ (6.0 g, 36.8 mmol) and filtered saturated aqueous KPF$_6$ (400 ml) were added to precipitate the crude complex. The dried precipitate was dissolved in 2:1 EtOH:MeCN (v/v), filtered, and rotary evaporated to dryness. Column chromatography was carried with Sephadex LH-20 resin; 100% MeCN was used as eluent. A second column chromatography was performed using silica gel, with 7:1:0.5 MeCN:KNO$_3$:H$_2$O as eluent. The silica gel column produced a pure product as determined by ESI MS analysis. Yield = 1.21 g (45%).

Calc. for C$_{48}$H$_{34}$F$_{10}$N$_8$O$_3$P$_2$RuS$_2$, C, 45.97; H, 2.73; N, 11.17; P, 4.94; S, 5.11. Found: C, 46.34; H, 2.38; N, 10.99; P, 5.52; S, 5.14. *m/z* (ESI, positive mode): 1055.00 (100%, [M – PF$_6$]$^+$). UV-visible spectrum (CH$_3$CN), $\lambda_{max.}$/nm (10^{-4} ε/M^{-1} cm^{-1}): 222 (7.1), 246 (6.6), 280 (7.8), 308 (7.6), 344 sh (4.1), 376 (2.7), and 466 (2.0).

Synthesis of [Ru(pbt)$_2$(tpphz)VO(sal-*L*-tryp)](PF$_6$)$_2$•6H$_2$O 3—[Ru(pbt)$_2$(tpphz)](PF$_6$)$_2$•3H$_2$O (0.450 g, 0.36 mmol) and [VO(sal-*L*-tryp)(H$_2$O)] (0.140 g, 0.36 mmol), ethanol (250 ml) and acetonitrile (100 ml) were mixed in a 500 ml round bottom flask, and the reaction mixture was refluxed for three hours with stirring under argon. The reaction mixture was rotary evaporated to dryness. The product was washed with ether and collected. Yield = 0.556 g (91%).

Calc. for C$_{66}$H$_{54}$F$_{12}$N$_{12}$O$_{10}$P$_2$RuS$_2$V, C, 47.15; H, 3.24; N, 10.00; P, 3.68; S, 3.81. Found: C, 47.08; H, 3.35; N, 9.70; P, 3.64; S, 3.67. *m/z* (ESI, positive mode): 660.65 (100%, [M – 2PF$_6$ + Na – 2H]$^+$). High resolution ESI MS: *m/z* = 1428.1033 (100%, [M – PF$_6$]$^+$). FT IR (ν/cm^{-1}): 3438 (m) (indolic NH), 1540 (m) (C-O), 1480 (m) (CO_2^- symmetric), 1616 (s) (CO_2^- asymmetric), 1583 (m) (C=N), 960 (s) (V=O), and 831 (vs) (PF_6^-). UV-visible spectrum (2:1 MeOH/CH$_3$CN (v/v)), $\lambda_{max.}$/nm (10^{-4} ε/M^{-1} cm^{-1}): 216 (11), 280 (9.0), 306 (7.2), 344 sh (2.8), and 466 (1.8).

Synthesis of [Ru(pbt)$_2$(phen$_2$DTT)VO(sal-*L*-tryp)](PF$_6$)$_2$•5H$_2$O 4—[Ru(pbt)$_2$(phen$_2$DTT)](PF$_6$)$_2$•1.5H$_2$O (0.450 g, 0.33 mmol) and [VO(sal-*L*-tryp)(H$_2$O)] (0.130 g, 0.33 mmol), ethanol (250 ml) and acetonitrile (100 ml) were mixed in a 500 ml round bottom flask, and the reaction mixture was refluxed for three hours with stirring under argon. The reaction mixture was rotary evaporated to dryness, and the product was washed with ether and collected. Yield = 0.533 g (90%).

Calc. for C$_{70}$H$_{62}$F$_{12}$N$_{10}$O$_{11}$P$_2$RuS$_4$V, C, 46.98; H, 3.49; N, 7.83; P, 3.46; S, 7.17. Found: C, 47.28; H, 3.57; N, 7.74; P, 3.12; S, 7.12. *m/z* (ESI, positive mode): 1554.00 (100%, [M – PF$_6$]$^+$). High resolution ESI MS: *m/z* = 1554.1086 (100%, [M – PF$_6$]$^+$). FT IR (ν/cm^{-1}): 3437 (m) (indolic NH), 1540 (m) (C-O), 1479 (m) (CO_2^- symmetric), 1620 (s) (CO_2^-

asymmetric), 1583 (m) (C=N), 956 (s) (V=O), and 837 (vs) (PF_6^-). UV-visible spectrum (2:1 MeOH/CH_3CN (v/v)), $\lambda_{max.}$/nm (10^{-4} ε/M^{-1} cm^{-1}): 224 (10), 264 (6.1), 326 (4.1), and 462 (1.3).

Preparation of [Ru(pbt)$_2$(tpphz)VO(sal-*L*-tryp)]Cl$_2$ and [Ru(pbt)$_2$(phen$_2$DTT)VO(sal-*L*-tryp)]Cl$_2$—Conversion of complex **3** into [Ru(pbt)$_2$(tpphz)VO(sal-*L*-tryp)]Cl$_2$: Complex **3** was dissolved in a minimum volume of CH_3CN, followed by an excess amount of [Bu_4N]Cl; then the resulting solution was rotary evaporated to leave a solid. Acetone was added to dissolve the excess [Bu_4N]Cl and [Bu_4N]PF_6 which was produced. [Ru(pbt)$_2$(tpphz)VO(sal-*L*-tryp)]Cl$_2$ was insoluble in acetone. The resulting mixture was filtered, and the residue was washed with acetone; then air-dried. The yield was quantitative. FT IR (ν/cm^{-1}): 1539 (m) (C-O), 1479 (m) (CO_2^- symmetric), 1616 (vs) (CO_2^- asymmetric), 1586 (m) (C=N), and 957 (s) (V=O).

Conversion of complex **4** into [Ru(pbt)$_2$(phen$_2$DTT)VO(sal-*L*-tryp)]Cl$_2$: Complex **4** and an excess amount of [Bu_4N]Cl were added to a round bottom flask containing 2:1 MeOH/MeCN (v/v) and acetone under argon. The mixture was warmed under argon with stirring until all solids dissolved totally. The resulting solution was rotary evaporated to leave a solid. Acetone was added to dissolve the excess [Bu_4N]Cl and [Bu_4N]PF_6 which was produced. [Ru(pbt)$_2$(phen$_2$DTT)VO(sal-*L*-tryp)]Cl$_2$ was insoluble in acetone. The resulting mixture was filtered, and the residue was washed with acetone; then air-dried. The yield was quantitative. FT IR (ν/cm^{-1}): 1540 (m) (C-O), 1479 (m) (CO_2^- symmetric), 1620 (vs) (CO_2^- asymmetric), 1586 (m) (C=N), and 955 (s) (V=O).

Supplementary Material

Refer to Web version on PubMed Central for supplementary material.

Acknowledgments

This research was supported in part by an appointment to the Student Research Participation Program at the U.S. Army Engineer Research and Development Center, Construction Engineering Research Laboratory, administered by the Oak Ridge Institute for Science and Education through an interagency agreement between the U.S. Department of Energy and ERDC-CERL. This work was also supported by the Mississippi INBRE funded by an IDeA award from the National Institute of General Medical Sciences of the National Institutes of Health (NIH) under grant number P20 GM103476. The authors also acknowledge the National Science Foundation (NSF) for funding our ESI and MALDI-ToF mass spectrometers (Grant CHE 0639208). We are also grateful for the use of our Bruker BioSpin EMXmicro ESR spectrometer, which was funded by the NSF CRIF:MU Award # 0741991. AAH appreciates funding from the Aubrey Keith Lucas and Ella Ginn Lucas Endowment for Faculty Excellence Award and ExxonMobil Research and Engineering Company. Funding from the Alliance for Graduate Education in Mississippi Summer Research Experience for Undergraduates (funded by the National Science Foundation, grant number HRD-0450362) for MG and JS is gratefully appreciated. JLW appreciates funding from the NIH, grant number R01CA140487, which helped in gathering data for this research.

We also acknowledge Dr. Aimin Liu and Ms. Fange Liu of Georgia State University for their assistance in acquiring two ESR spectra for us in liquid helium. We also acknowledge Ms. Baobin Kang of the University of Southern Mississippi for acquiring DIC and phase contrast image using a Zeiss LSM510 META confocal imaging system.

References

1. Jemal A, Siegel R, Xu J, Ward E. CA Cancer J. Clin. 2010; 60:277. [PubMed: 20610543]

2. Siegel R, Naishadham D, Jemal A. CA Cancer J. Clin. 2012; 62:10. [PubMed: 22237781]
3. Wong E, Giandomenico CM. Chem. Rev. 1999; 99:2451. [PubMed: 11749486]
4. Galanski M, Arion VB, Jakupec MA, Keppler BK. Curr. Pharm. Des. 2003; 9:2078. [PubMed: 14529417]
5. Jakupec MA, Galanski M, Keppler BK. Rev. Physiol., Biochem. Pharm. 2003; 146:1.
6. Ott I, Gust R. Archiv der Pharmazie - Chemistry in Life Sciences. 2007; 340:117.
7. Dougherty TJ, Gomer CJ, Henderson BW, Jori G, Kessel D, Korbelik M, Moan J, Peng Q. J. Natl. Cancer Inst. 1998; 90:889. [PubMed: 9637138]
8. MacDonald IJ, Dougherty TJ. J. Porphyrins Phthalocyanines. 2001; 5:105.
9. Ackroyd R, Kelty C, Brown N, Reed M. Photochem. Photobiol. 2001; 74:656. [PubMed: 11723793]
10. Bonnett, R. Chemical Aspects of Photodynamic Therapy. Taylor and Francis, Inc.; 2000.
11. Sharman WM, Allen CM, van Lier JE. Drug Discovery Today. 1999; 4:507. [PubMed: 10529768]
12. Capella MAM, Capella LS. J. Biomed. Sci. 2003; 10:361. [PubMed: 12824695]
13. Fu PKL, Bradley PM, Turro C. Inorg. Chem. 2001; 40:2476. [PubMed: 11350221]
14. Armitage B. Chem. Rev. 1998; 98:1171. [PubMed: 11848929]
15. Clarke MJ. Coord. Chem. Rev. 2003; 203:209.
16. Clarke MJ, Zhu F, Frasca DR. Chem. Rev. 1999; 99:2511. [PubMed: 11749489]
17. Brabec V, Kasparkova J. Metal Compounds Cancer Chem. 2005:187.
18. Pongratz M, Schluga P, Jakupec MA, Arion VB, Hartinger CG, Allmaier G, Keppler BK. J. Analyt. Atomic Spect. 2004; 19:46.
19. Timerbaev AR, Hartinger CG, Aleksenko SS, Keppler BK. Chem. Rev. 2006; 106:2224. [PubMed: 16771448]
20. Vock CA, Ang WH, Scolaro C, Phillips AD, Lagopoulos L, Juillerat-Jeanneret L, Sava G, Scopelliti R, Dyson PJ. J. Med. Chem. 2007; 50:2166. [PubMed: 17419606]
21. Sava G, Bergamo A. Int. J. Oncol. 2000; 17:353. [PubMed: 10891547]
22. Scolaro C, Bergamo A, Brescacin L, Delfino R, Cocchietto M, Laurenczy G, Geldbach TJ, Sava G, Dyson PJ. J. Med. Chem. 2005; 48:4161. [PubMed: 15943488]
23. Silva, D. d. O. Anti-Cancer Agents Med. Chem. 2010; 10:312.
24. Hartinger CG, Jakupec MA, Zorbas-Seifried S, Groessl M, Egger A, Berger W, Zorbas H, Dyson PJ, Keppler BK. Chem. Biodivers. 2008; 5:2140. [PubMed: 18972504]
25. Jakupec MA, Galanski M, Arion VB, Hartinger CG, Keppler BK. Dalton Trans. 2008:183. [PubMed: 18097483]
26. Groessl M, Tsybin YO, Hartinger CG, Keppler BK, Dyson PJ. J. Biol. Inorg. Chem. 2010; 15:677. [PubMed: 20213306]
27. Bratsos I, Jedner S, Gianferrara T, Alessio E. Chimia. 2007; 61:692.
28. Holder AA, Zigler DF, Tarrago-Trani MT, Storrie B, Brewer KJ. Inorg. Chem. 2007; 46:4760. [PubMed: 17488069]
29. Holder AA, Swavey S, Brewer KJ. Inorg. Chem. 2004; 43:303. [PubMed: 14704081]
30. Davia K, King D, Hong Y, Swavey S. Inorg. Chem. Commun. 2008; 11:584.
31. Narra M, Elliott P, Swavey S. Inorg. Chim. Acta. 2006; 359:2256.
32. Araki K, Silva CA, Toma HE, Catalani LH, Medeiros MH, Di Mascio P. J. Inorg. Biochem. 2000; 78:269. [PubMed: 10857906]
33. Schmitt F, Govindaswamy P, Suess-Fink G, Ang WH, Dyson PJ, Juillerat-Jeanneret L, Therrien B. J. Med. Chem. 2008; 51:1811. [PubMed: 18298056]
34. Gianferrara T, Bergamo A, Bratsos I, Milani B, Spagnul C, Sava G, Alessio E. J. Med. Chem. 2010; 53:4678. [PubMed: 20491441]
35. Rani-Beeram S, Meyer K, McCrate A, Hong Y, Nielsen M, Swavey S. Inorg.c Chem. 2008; 47:11278.
36. Higgins SLH, Tucker AJ, Winkel BSJ, Brewer KJ. Chem. Commun. 2012; 48:67.
37. Wachter E, Heidary DK, Howerton BS, Parkin S, Glazer EC. Chem. Commun. 2012; 48:9649.
38. Chakravarty AR, Roy M. Prog. Inorg. Chem. 2012; 57:119.

39. Butenko N, Tomaz Ana I, Nouri O, Escribano E, Moreno V, Gama S, Ribeiro V, Telo Joao P, Pesssoa Joao C, Cavaco I. J. Inorg. Biochem. 2009; 103:622. [PubMed: 19230978]
40. Kuwahara J, Suzuki T, Sugiura Y. Biochem. Biophys. Res. Commun. 1985; 129:368. [PubMed: 2409964]
41. Sasmal PK, Patra AK, Nethaji M, Chakravarty AR. Inorg. Chem. 2007; 46:11112. [PubMed: 18020327]
42. Banerjee S, Hussain A, Prasad P, Khan I, Banik B, Kondaiah P, Chakravarty AR. Eur. J. Inorg. Chem. 2012; 2012:3899.
43. Banerjee S, Prasad P, Hussain A, Khan I, Kondaiah P, Chakravarty AR. Chem. Commun. 2012; 48:7702.
44. Crans DC, Smee JJ, Gaidamauskas E, Yang L. Chem. Rev. 2004; 104:849. [PubMed: 14871144]
45. Thompson KH, McNeill JH, Orvig C. Chem. Rev. 1999; 99:2561. [PubMed: 11749492]
46. Sakurai H. Biomed. Res. Trace Elements. 2007; 18:241.
47. Sakurai H. ACS Symposium Series. 2007; 974:110.
48. Sakurai H, Yoshikawa Y, Yasui H. Chem. Soc. Rev. 2008; 37:2383. [PubMed: 18949111]
49. Li M, Ding W, Smee JJ, Baruah B, Willsky GR, Crans DC. Biometals. 2009; 22:895. [PubMed: 19404749]
50. D'Cruz OJ, Uckun FM. Expert Opin. Invest. Drugs. 2002; 11:1829–1836.
51. Fichtner I, Claffey J, Deally A, Gleeson B, Hogan M, Markelova MR, Mueller-Bunz H, Weber H, Tacke M. J. Organomet. Chem. 2010; 695:1175.
52. Rehder, D. Bioinorganic Vanadium Chemistry. Editon edn.. John Wiley & Sons, Ltd.; Chichester, West Sussex: 2008. p. 176
53. Evangelou A. Crit. Rev. Oncol./Hematol. 2002; 42:249.
54. Lewis NA, Liu F, Seymour L, Magnusen A, Erves TR, Arca JF, Beckford FA, Venkatraman R, González-Sarrías A, Fronczek FR, VanDerveer DG, Seeram NP, Liu A, Jarrett WL, Holder AA. Eur. J. Inorg. Chem. 2012; 2012:664. [PubMed: 23904789]
55. Lewis, NA. M.S. thesis. The University of Southern Mississippi; 2011.
56. Demirci TB, Koseoglu Y, Guner S, Ulkuseven B. Cent. Eur. J. Chem. 2006; 4:149.
57. Zhang H, Thomas R, Oupicky D, Peng F. J. Biol. Inorg. Chem. 2008; 13:47. [PubMed: 17909866]
58. Mendes IC, Botion LM, Ferreira AVM, Castellano EE, Beraldo H. Inorg. Chim. Acta. 2009; 362:414.
59. Pessoa JC, Cavaco I, Correia I, Tomaz I, Duarte T, Matias PM. J. Inorg. Biochem. 2000; 80:35. [PubMed: 10885461]
60. Yuan C, Lu L, Gao X, Wu Y, Guo M, Li Y, Fu X, Zhu M. J. Biol. Inorg. Chem. 2009; 14:841. [PubMed: 19290551]
61. Ebel M, Rehder D. Inorg. Chim. Acta. 2003; 356:210.
62. Garribba E, Lodyga-Chruscinska E, Micera G, Panzanelli A, Sanna D. Eur. J. Inorg. Chem. 2005:1369.
63. Micera G, Garribba E. J. Comput. Chem. 2011; 32:2822. [PubMed: 21735449]
64. Micera G, Garribba E. Dalton Trans. 2009:1914. [PubMed: 19259560]
65. Micera G, Pecoraro VL, Garribba E. Inorg. Chem. 2009; 48:5790. [PubMed: 19449891]
66. Richter MM, Brewer KJ. Inorg. Chem. 1993; 32:2827.
67. Downard AJ, Honey GE, Phillips LF, Steel PJ. Inorg. Chem. 1991; 30:2259.
68. Guillo P, Hamelin O, Loiseau F, Pecaut J, Menage S. Dalton Trans. 2010; 39:5650. [PubMed: 20485756]
69. Kianfar AH, Mohebbi S. J. Iran. Chem. Soc. 2007; 4:215.
70. Maia, P. I. d. S.; Pavan, FR.; Leite, CQF.; Lemos, SS.; de, SGF.; Batista, AA.; Nascimento, OR.; Ellena, J.; Castellano, EE.; Niquet, E.; Deflon, VM. Polyhedron. 2009; 28:398.
71. Crans DC, Holder AA, Saha TK, Prakash GK, Yousufuddin M, Kultyshev R, Ismail R, Goodman MF, Borden J, Florián F. Inorg. Chem. 2007; 46:6723–6732. [PubMed: 17628058]
72. Crans DC. Comments Inorg. Chem. 1994; 16:1.

73. Chasteen ND. Biol. Magn. Reson. 1981; 3:53.
74. Liboiron BD, Thompson KH, Hanson GR, Lam E, Aebischer N, Orvig C. J. Am. Chem. Soc. 2005; 127:5104. [PubMed: 15810845]
75. Benitez J, Cavalcanti d. Q. A. Correia I, Alves MA, Alexandre-Moreira MS, Barreiro EJ, Lima LM, Varela J, Gonzalez M, Cerecetto H, Moreno V, Pessoa JC, Gambino D. Eur. J. Med. Chem. 2013; 62:20. [PubMed: 23353731]
76. Chan WS, Marshall JF, Svensen R, Phillips D, Hart IR. Photochem. Photobiol. 1987; 45:757. [PubMed: 3628498]
77. Taquet, J.-p.; Frochot, C.; Manneville, V.; Barberi-Heyob, M. Curr. Med. Chem. 2007; 14:1673. [PubMed: 17584072]
78. Giuntini F, Raoul Y, Dei D, Municchi M, Chiti G, Fabris C, Colautti P, Jori G, Roncucci G. Tetrahedron Lett. 2005; 46:2979.
79. Cauchon N, Tian H, Langlois R. j. La Madeleine C, Martin S, Ali H, Hunting D, van Lier JE. Bioconj. Chem. 2004; 16:80.
80. Mahon KP Jr. Ortiz-Meoz RF, Prestwich EG, Kelley SO. Chem. Commun. 2003:1956.
81. Patra AK, Bhowmick T, Ramakumar S, Nethaji M, Chakravarty AR. Dalton Trans. 2008:6966. [PubMed: 19050783]
82. Kawashima T, Ohkuboa K, Fukuzumi S. Org. Biomol. Chem. 2010; 8:994. [PubMed: 20165787]
83. Shawn S, Matthew T. Porphyrin and Phthalocyanine Photosensitizers as PDT Agents: A New Modality for the Treatment of Melanoma. 2013
84. Williams JL, Ji P, Ouyang N, Liu X, Rigas B. Carcinogenesis. 2008; 29:390. [PubMed: 18174252]
85. Lyon D, Walter J, Starkweather A, Schubert C, McCain N. BMC Research Notes. 2011; 4:156. [PubMed: 21615916]
86. Sucher R, Kurz K, Weiss G, Margreiter R, Fuchs D, Brandacher G. Int. J. Tryptophan Res. 2010; 3:113. [PubMed: 22084593]
87. Dotsenko IA, Curtis M, Samoshina NM, Samoshin VV. Tetrahedron. 2011; 67:7470.
88. Bolger J, Gourdon A, Ishow E, Launay J-P. Inorg. Chem. 1996; 35:2937.
89. Cropek DM, Metz A, Muller AM, Gray HB, Horne T, Horton DC, Poluektov O, Tiede DM, Weber RT, Jarrett WL, Phillips JD, Holder AA. Dalton Trans. 2012; 41:13060. [PubMed: 23001132]
90. Weber JH, Busch DH. Inorg. Chem. 1965; 4:469.

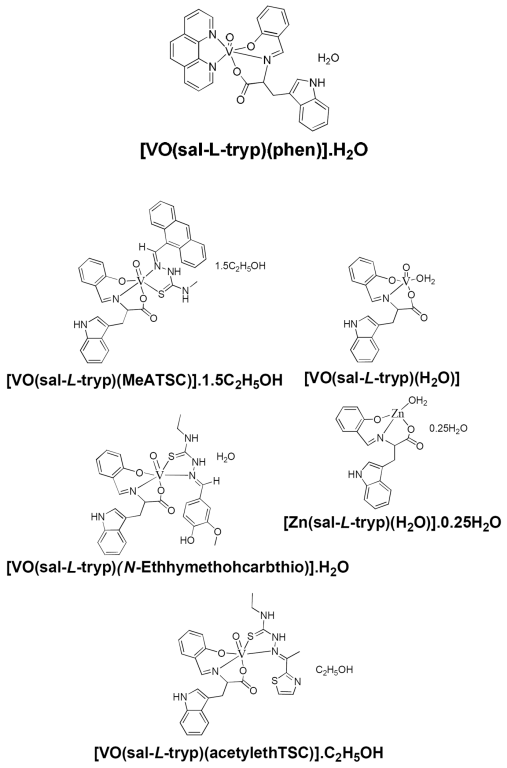

Figure 1.

The structures of [VO(sal-*L*-tryp)(H_2O)], [VO(sal-*L*-tryp)(phen)]•H_2O, [VO(sal-*L*-tryp)(MeATSC)]•1.5C_2H_5OH, [VO(sal-*L*-tryp)(*N*-Ethhymethohcarbthio)]•H_2O, [VO(sal-*L*-tryp)(acetylethTSC)]•C_2H_5OH, and [Zn(sal-*L*-tryp)(H_2O)]•0.25H_2O.

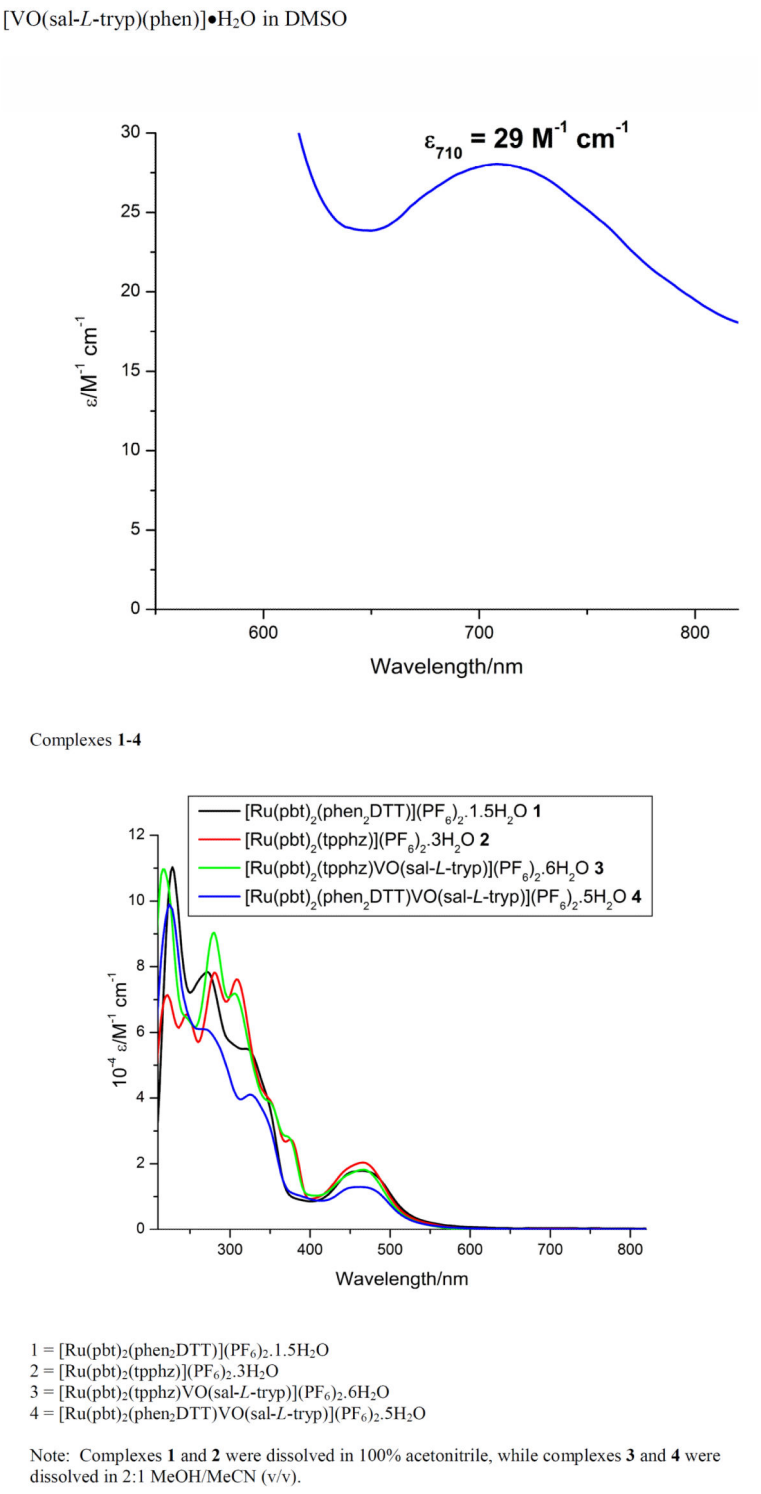

Figure 2.

The UV-visible spectra of [VO(sal-*L*-tryp)(phen)]•H_2O and the synthesised complexes. [VO(sal-*L*-tryp)(phen)]•H_2O in DMSO

[VO(sal-*L*-tryp)(phen)]•H_2O

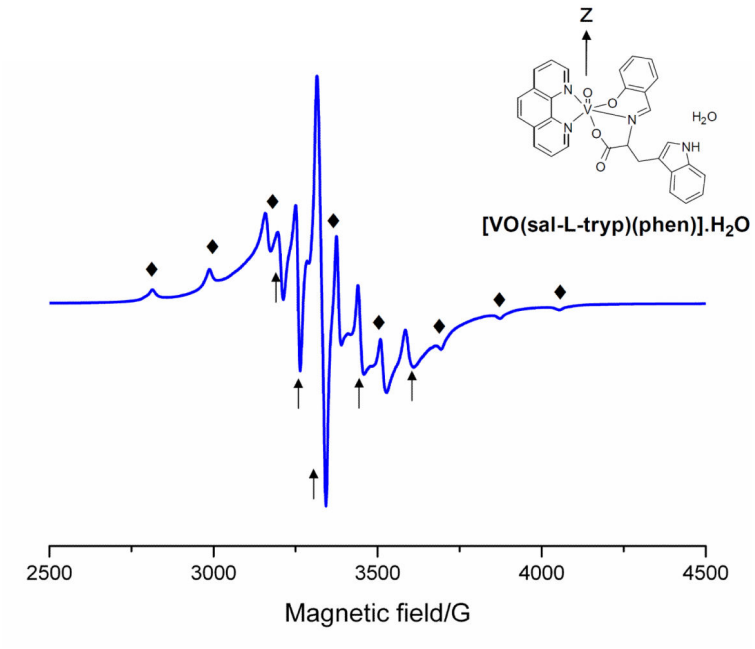

Complex **3**

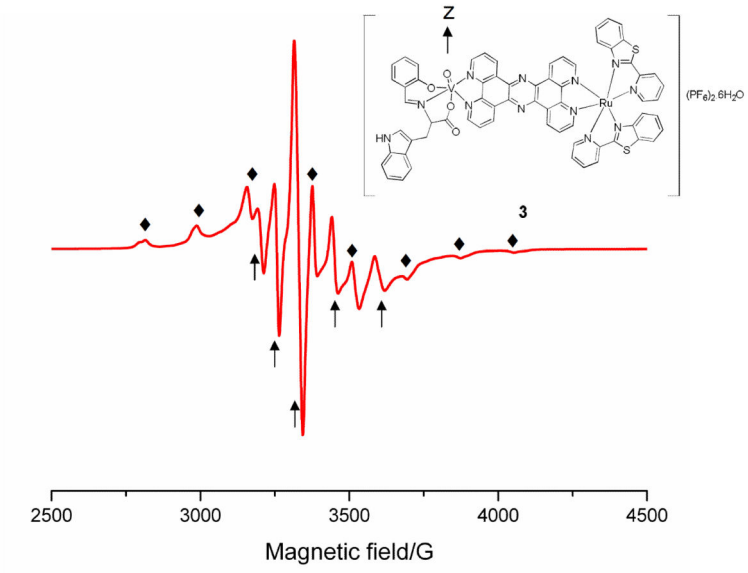

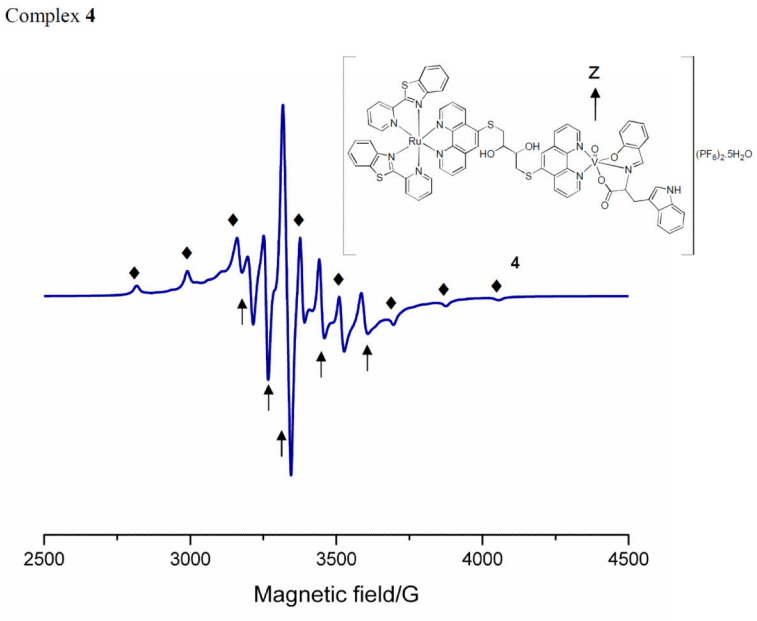

Figure 3.

Anisotropic axial ESR spectra of [VO(sal-*L*-tryp)(phen)]•H_2O, complex **3**, and complex **4** in DMSO at 10 K. [complex] = 10 mM. Instrument settings were as follows: centre field = 3360.00 G, sweep width = 4000.00 G, microwave frequency = 9.38 GHz, microwave power = 2.0 mW, modulation frequency = 100 kHz, modulation amplitude = 4.00 G, modulation phase = 0°, time constant = 328 ms, conversion time = 60.00 ms, and sweep time = 600 s. The diamonds indicate the eight components of $A_{\|}$ (the parallel hyperfine coupling constant; parallel defined by the *z* direction, which is the direction of the magnetic field). The arrows indicate the five inner component of the A_{τ}.

[complex] = 1.0 mM, supporting electrolyte = 0.10 mM tetra-*n*-butylammonium hexafluorophosphate (TBAP). All cyclic voltammetric measurements were carried out with a three-electrode system consisting of a working electrode = platinum, a platinum wire auxiliary electrode, and reference electrode = Ag/Ag^{+} (0.01 M $AgNO_3$ and 0.10 M TBAP in acetonitrile). Scan rate = 100 mV s^{-1}.

[VO(sal-*L*-tryp)(phen)]•H_2O

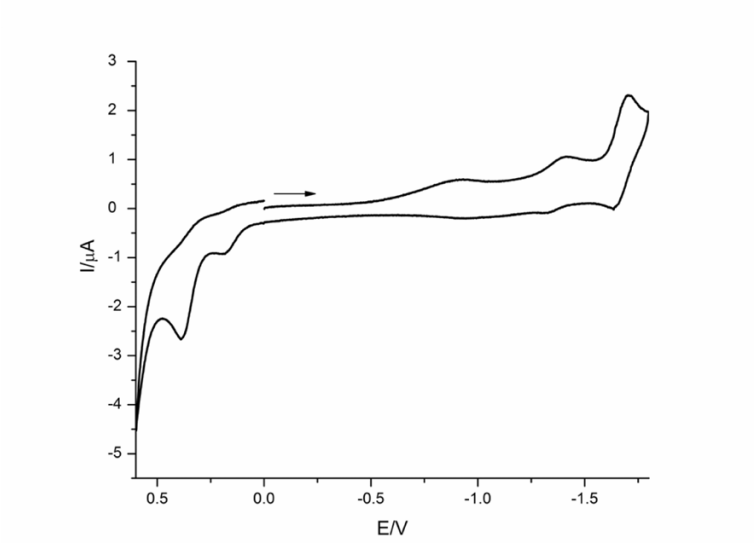

Complex **1**

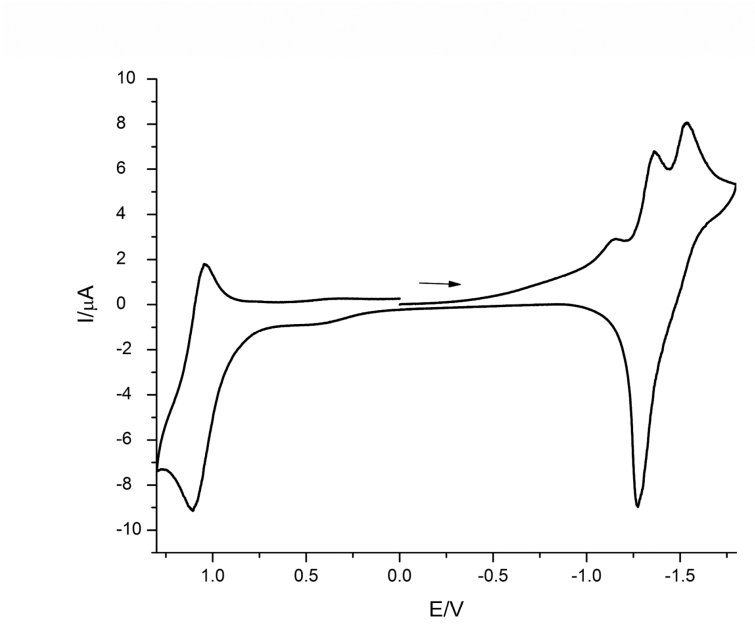

Complex **2**

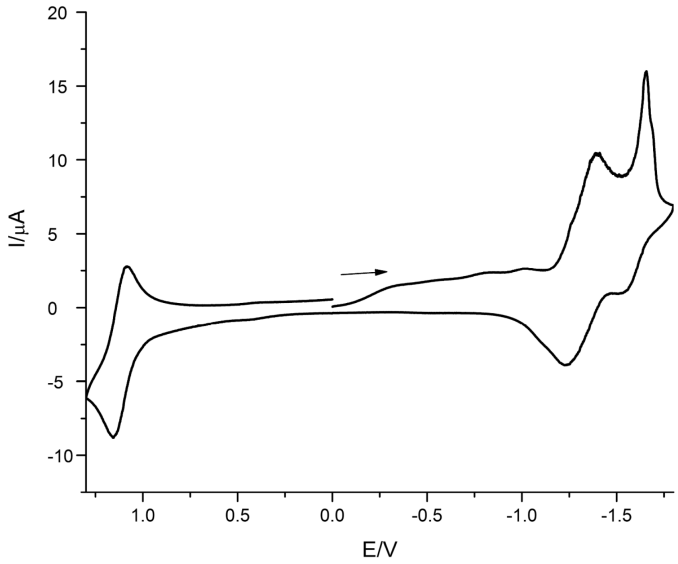

Complex **3**

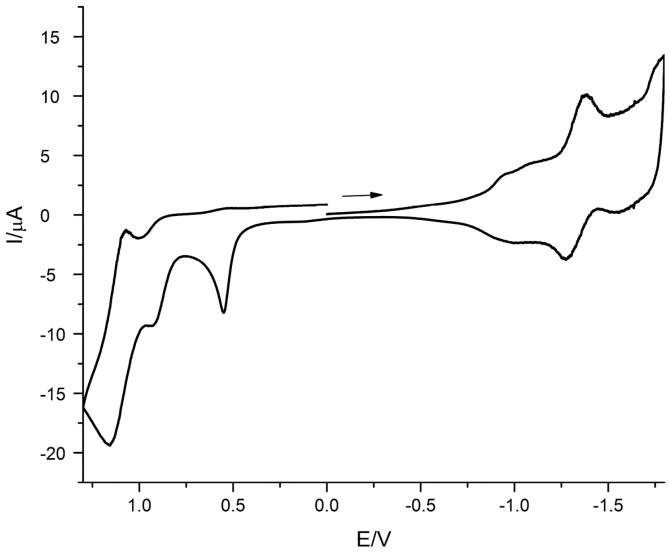

Complex **4**

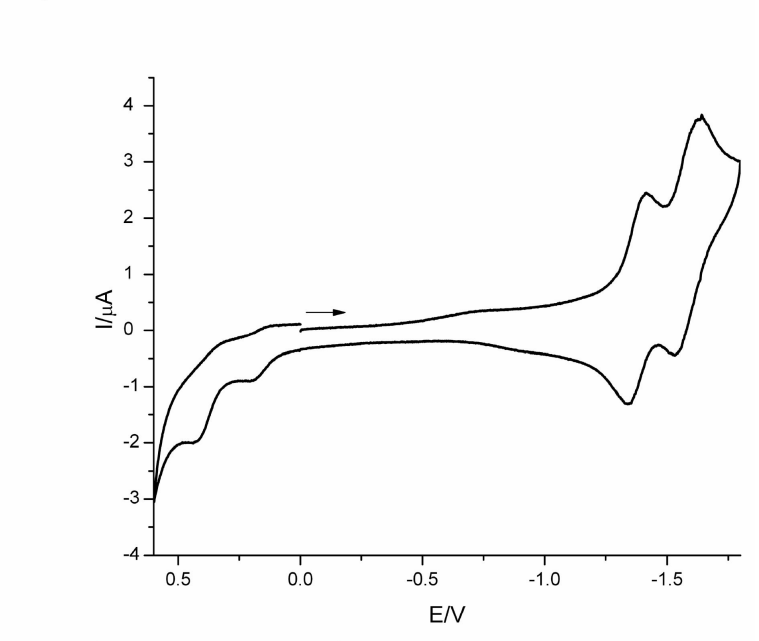

In water

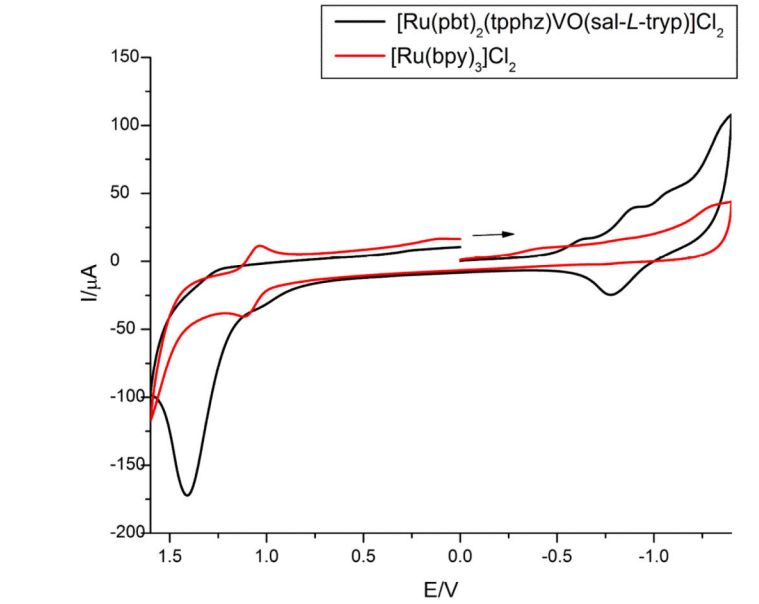

Figure 4.

Cyclic voltammograms of [VO(sal-*L*-tryp)(phen)]•H_2O and complexes **1**–**4** in their respective solvent.

Complexes **1**, **2**, and **3** were recorded in CH_3CN, while [VO(sal-*L*-tryp)(phen)]•H_2O and complex 4 were recorded in DMSO.

4.0 mM [Ru(pbt)$_2$(tpphz)VO(sal-*L*-tryp)]Cl$_2$

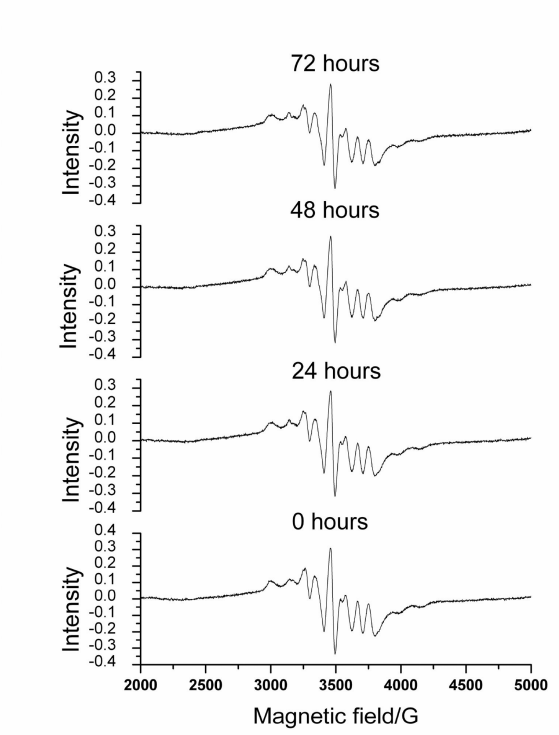

4.0 mM [Ru(pbt)$_2$(phen$_2$DTT)VO(sal-*L*-tryp)]Cl$_2$

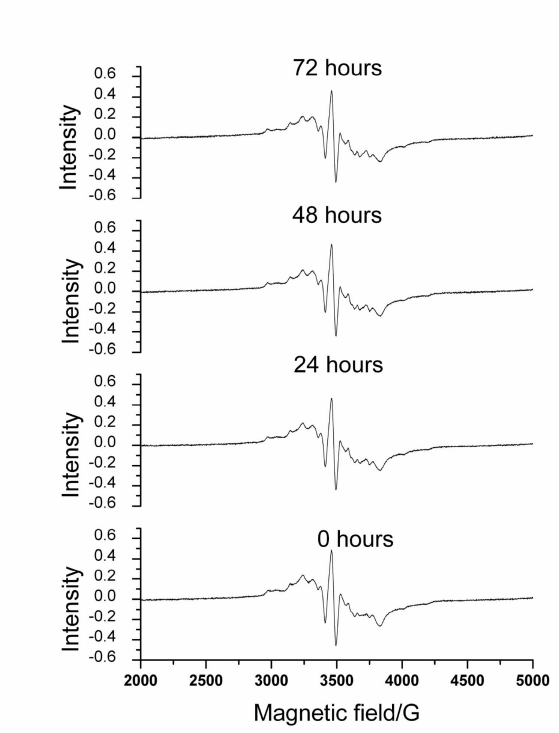

4.0 mM $VOSO_4$ in 0.1 M H_2SO_4. Instrument settings were as follows: centre field = 3520 G, sweep width = 2000 G, microwave frequency = 9.80 GHz, microwave power = 0.331 mW, modulation frequency = 100 kHz, modulation amplitude = 10.0 G, modulation phase = 0°, time constant = 40.96 ms, conversion time = 40 ms, and sweep time = 40.96 s.

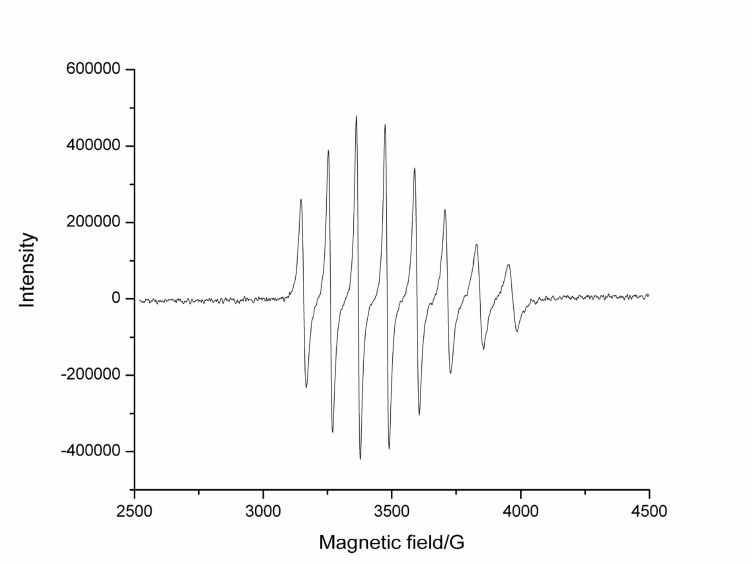

B. ^{51}V NMR spectra.
4.0 mM $[Ru(pbt)_2(tpphz)VO(sal\text{-}L\text{-}tryp)]Cl_2$

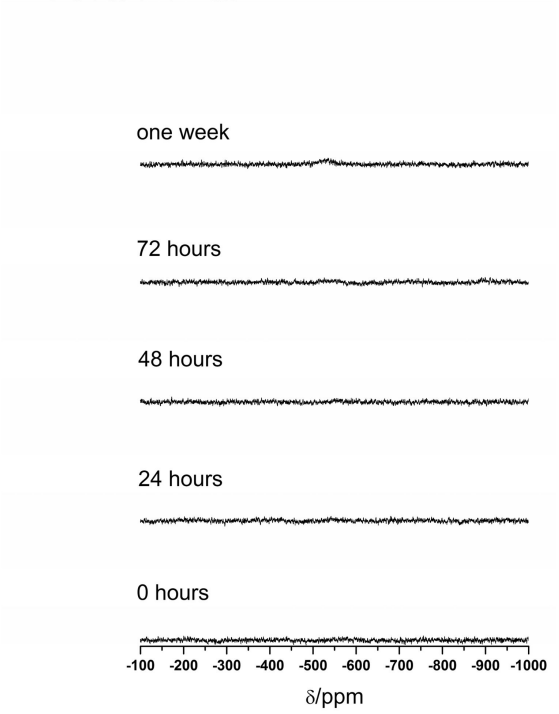

4.0 mM [Ru(pbt)$_2$(phen$_2$DTT)VO(sal-*L*-tryp)]Cl$_2$

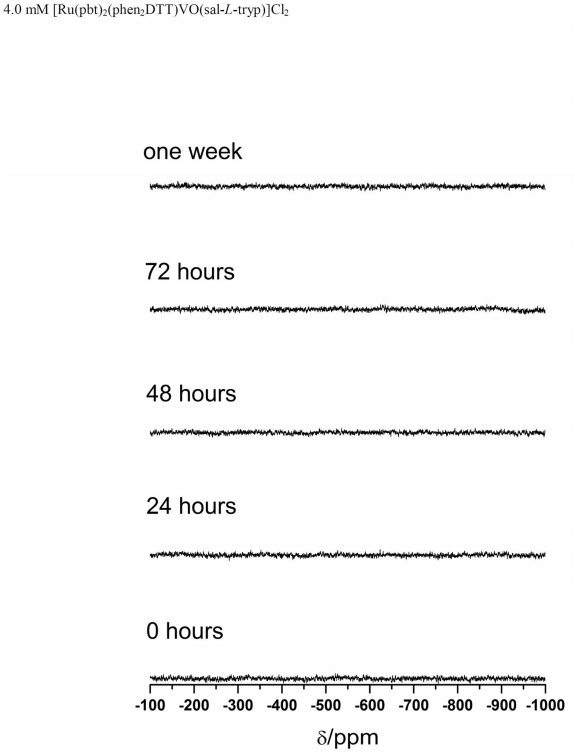

One week, 8192 scans. [Ru(pbt)$_2$(tpphz)VO(sal-*L*-tryp)]Cl$_2$, [Ru(pbt)$_2$(phen$_2$DTT)VO(sal-*L*-tryp)]Cl$_2$, and NaVO$_3$.

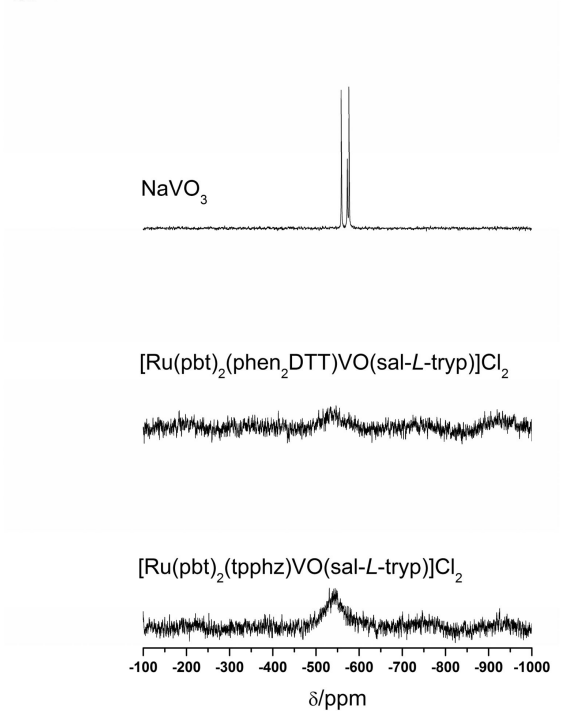

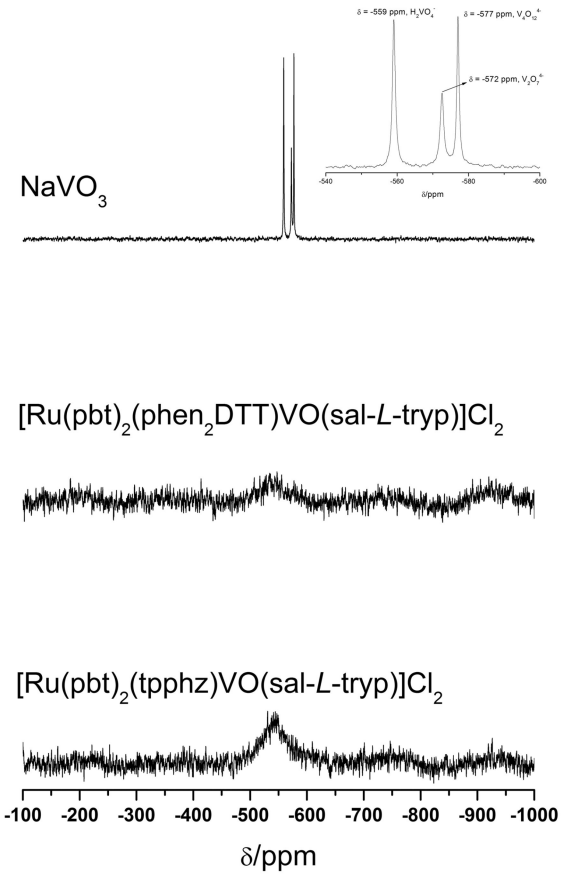

4.0 mM $NaVO_3$

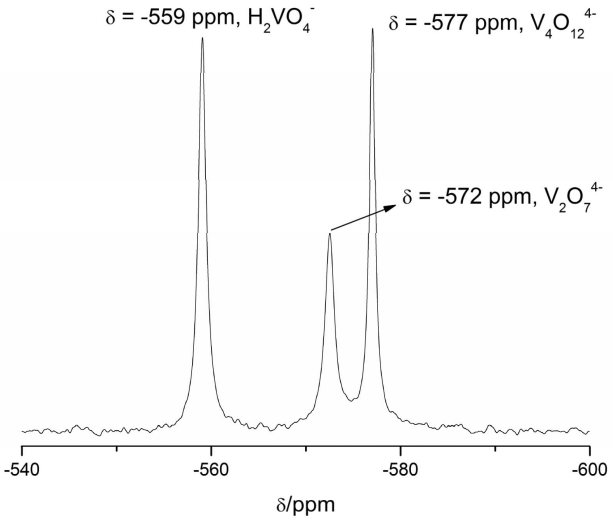

Figure 5.

ESR and ^{51}V NMR spectra of the respective complexes in water at room temperature. **A. ESR spectra.** [complex] = 4.0 mM and pH = 7.19. Parameters: Microwave frequency = 9.783 GHz, centre of field = 3500 G, sweep width = 3000 G, microwave power = 10 mW, sweep time = 5 minutes (4 averages), and modulation amplitude = 10 G.

$Na_4[Co(tspc)(H_2O)_2]$/HFF

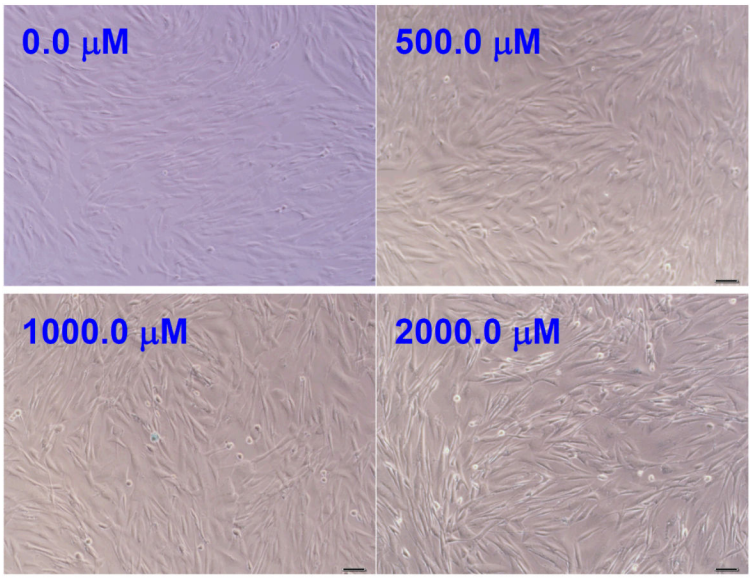

[VO(sal-*L*-tryp)(phen)]•H_2O/HFF

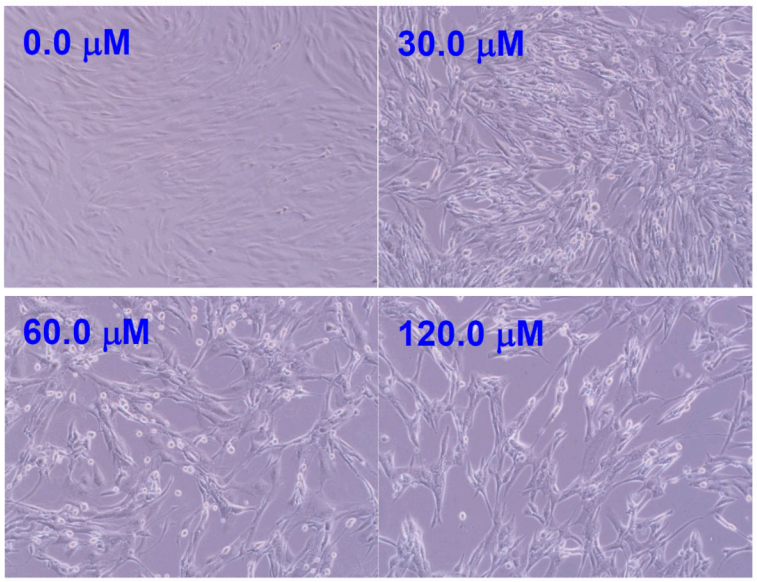

[Ru(pbt)$_2$(tpphz)VO(sal-*L*-tryp)]Cl$_2$/HFF

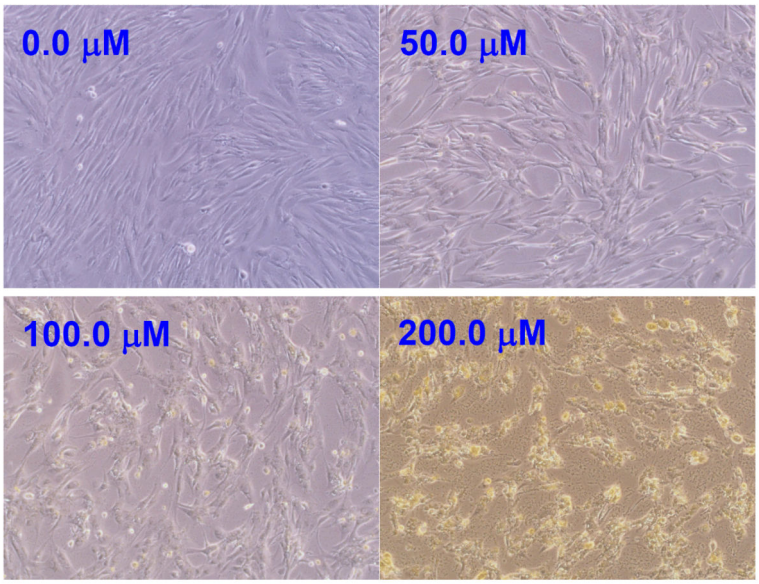

[Ru(pbt)$_2$(phen$_2$DTT)VO(sal-*L*-tryp)]Cl$_2$/HFF

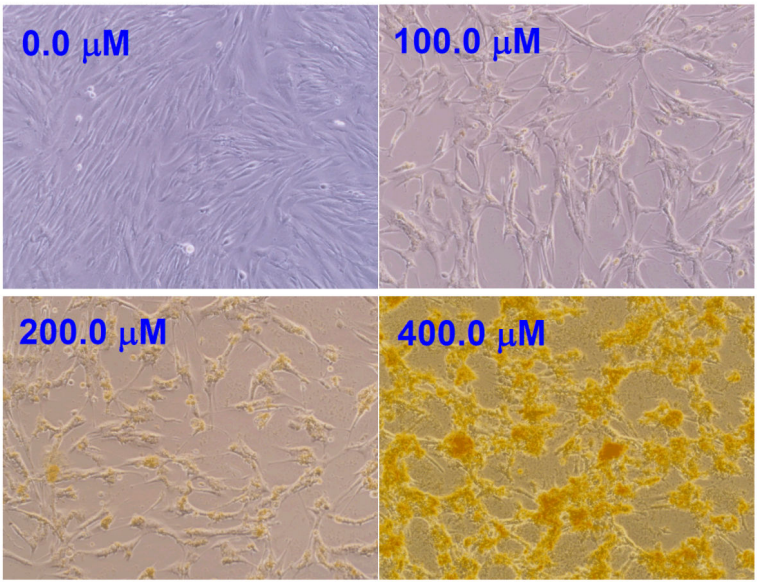

$Na_4[Co(tspc)(H_2O)_2]$/A431

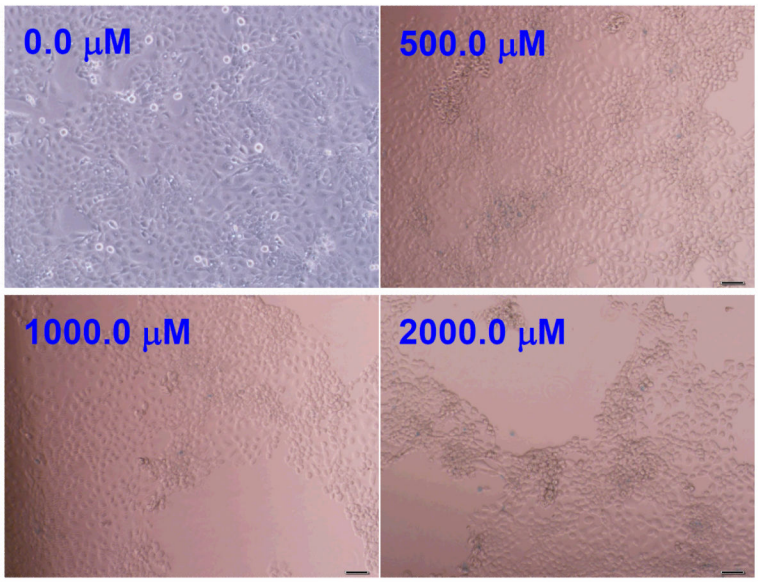

[VO(sal-*L*-tryp)(phen)]•H_2O/A431

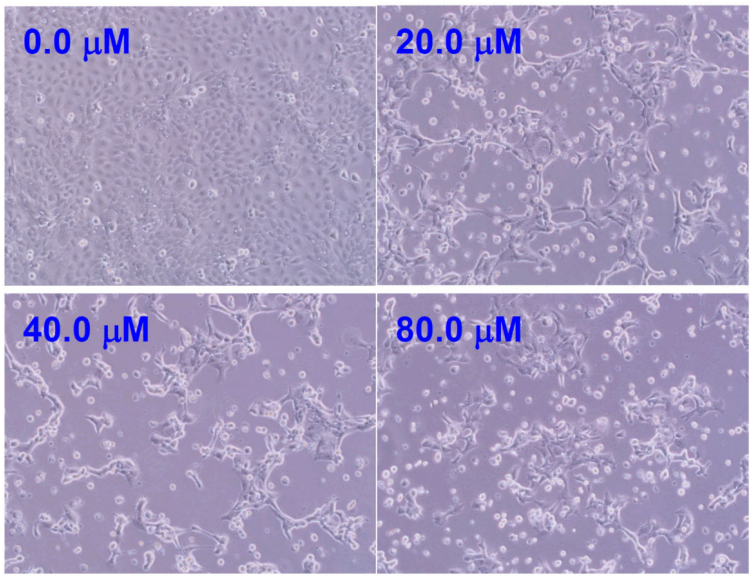

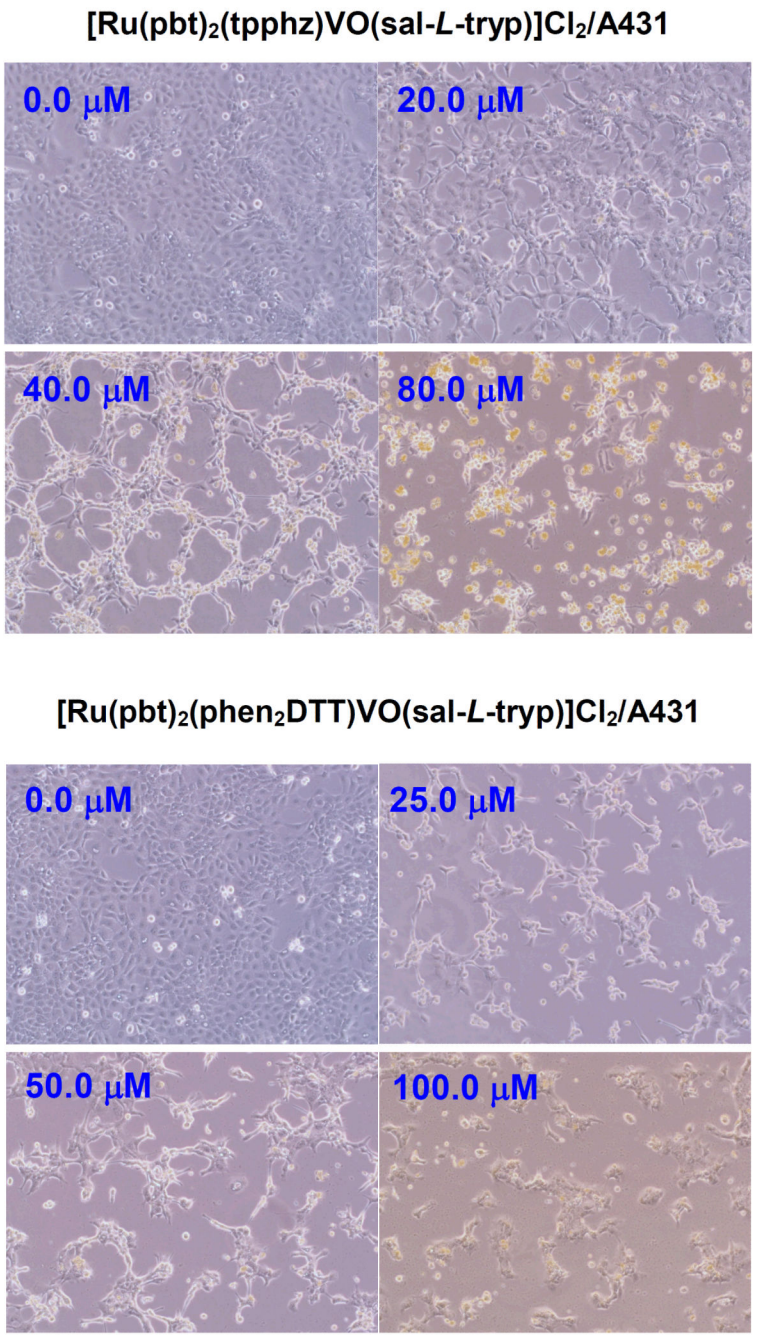

Figure 6.

Phase-contrast microscope images of A431, human epidermoid carcinoma cells and HFF, human skin fibroblast cells incubated in the dark for 24 hours in the presence of different concentrations of the listed compound. Magnification = 10×.

A. Dark toxicity with [Ru(pbt)$_2$(tpphz)VO(sal-*L*-tryp)]Cl$_2$

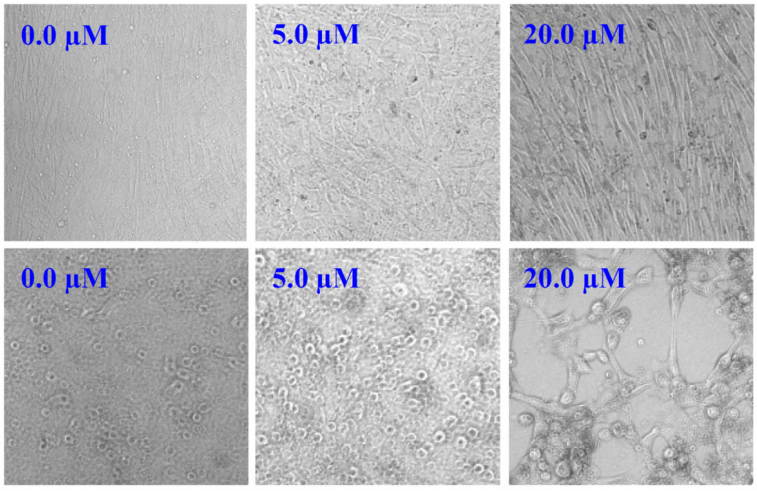

B. Light toxicity with [Ru(pbt)$_2$(tpphz)VO(sal-*L*-tryp)]Cl$_2$

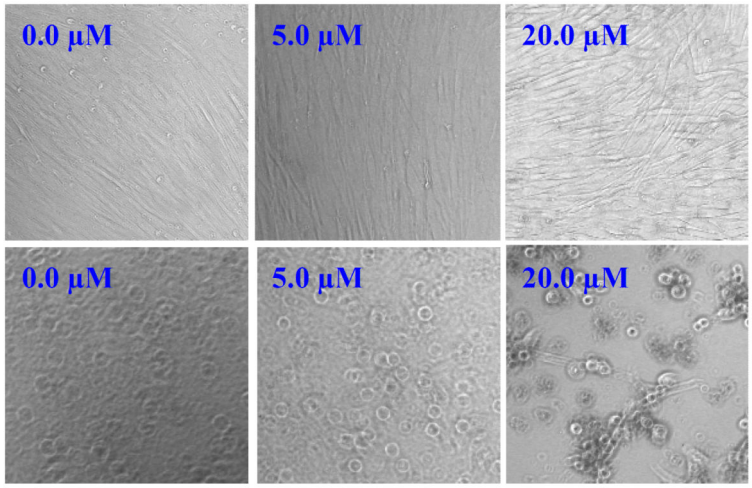

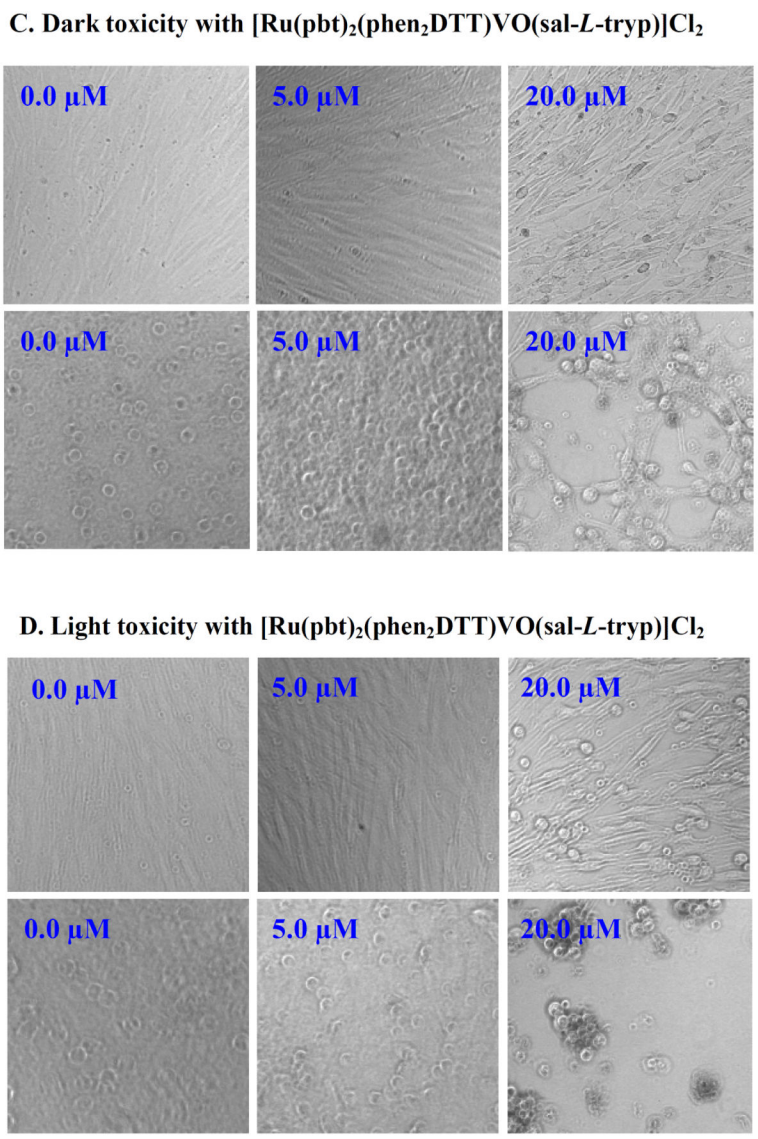

Figure 7.

Phase contrast image of HFF (upper panel) and A431 cells (lower panel). A (dark) and B (light) toxicity with $[Ru(pbt)_2(tpphz)VO(sal\text{-}L\text{-}tryp)]Cl_2$. C (dark) and D (light) toxicity with $[Ru(pbt)_2(phen_2DTT)VO(sal\text{-}L\text{-}tryp)]Cl_2$. Magnification = 10×

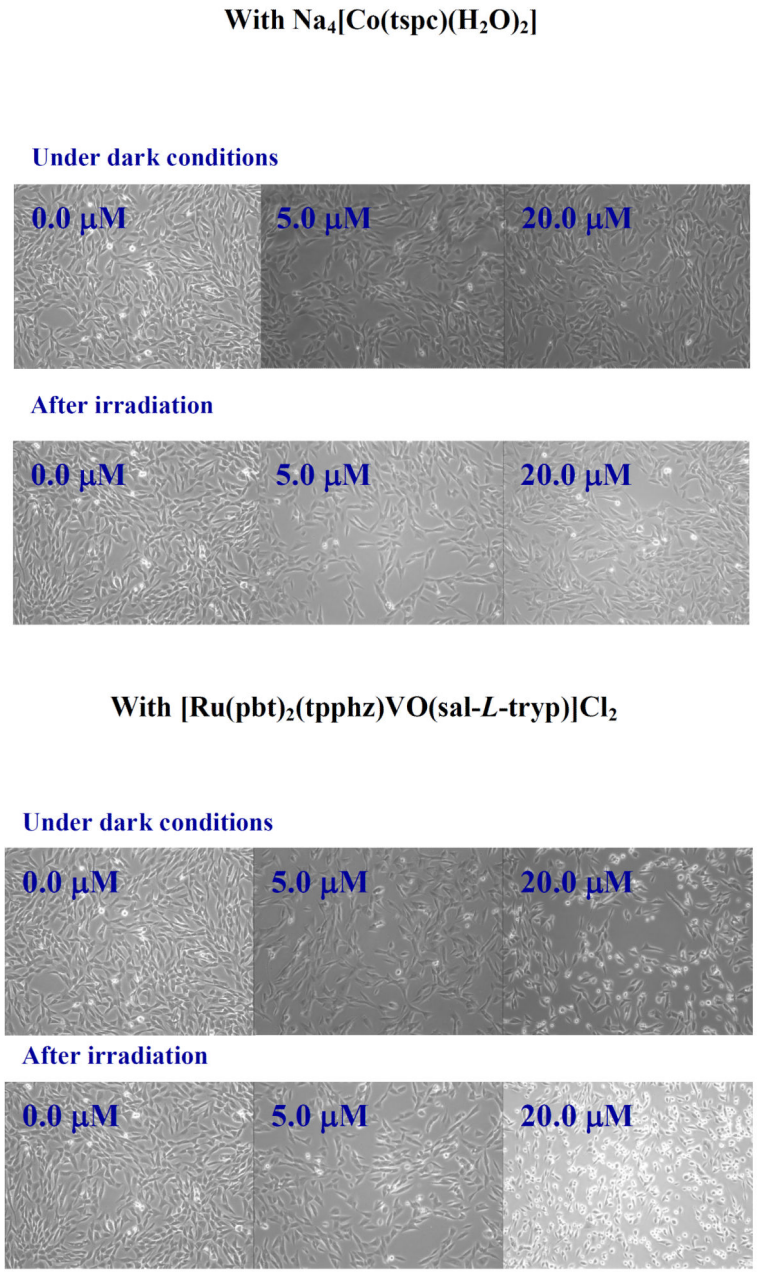

Figure 8.

Phase-contrast microscope images of amelanotic malignant melanoma cells. Magnification = 10×.

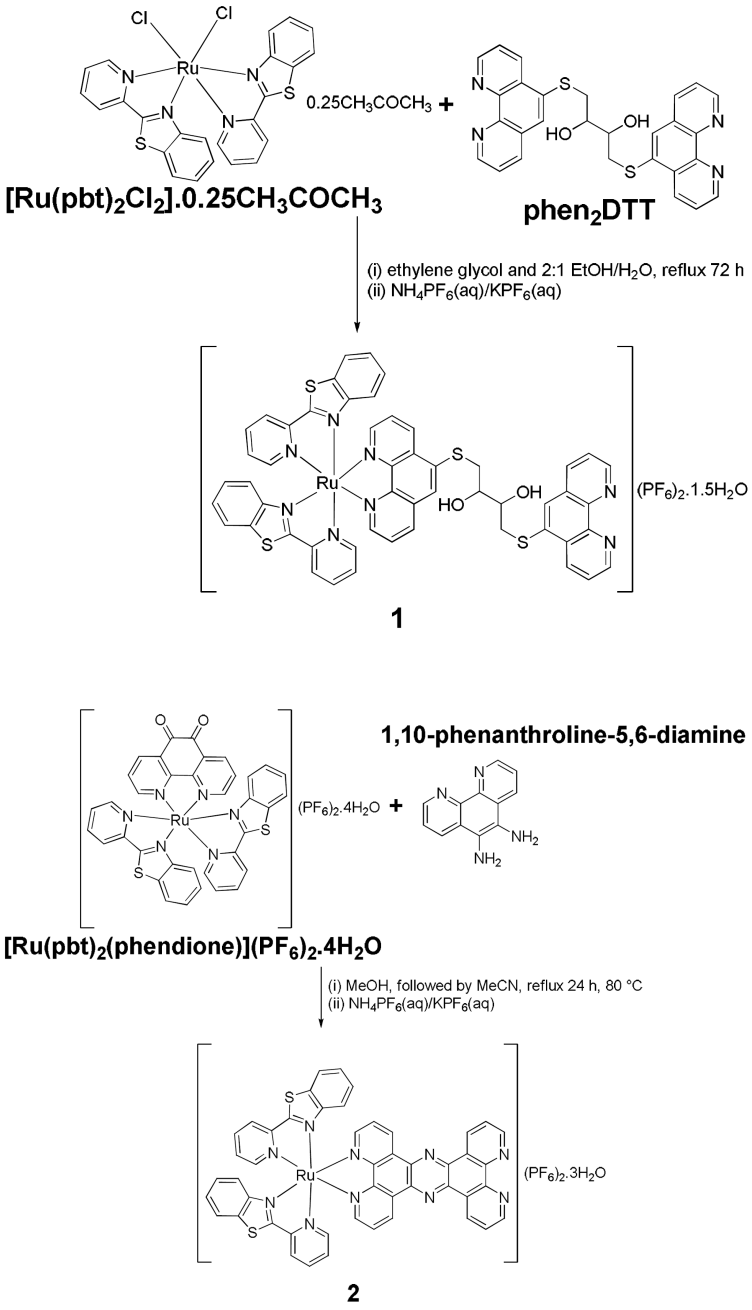

Scheme 1.
Synthesis of complexes **1** and **2**.

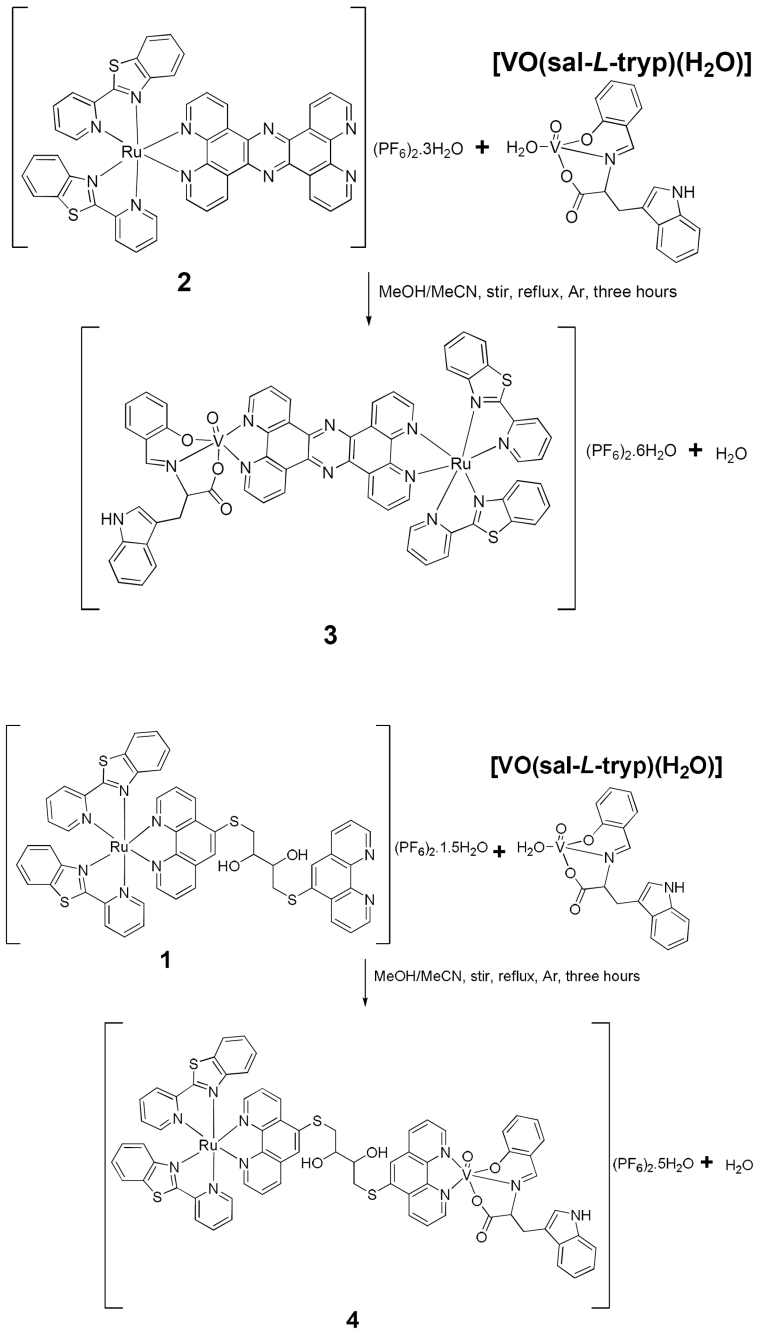

Scheme 2.
Synthesis of complexes **3** and **4**.

Table 1

UV-visible spectroscopic data of complexes **1**–**4** in the respective solvents.

Complex	λ_1/nm	$10^{-4}\ \varepsilon_1/M^{-1}\ cm^{-1}$	λ_2/nm	$10^{-4}\ \varepsilon_2/M^{-1}\ cm^{-1}$	λ_3/nm	$10^{-4}\ \varepsilon_3/M^{-1}\ cm^{-1}$	λ_4/nm	$10^{-4}\ \varepsilon_4/M^{-1}\ cm^{-1}$	λ_5/nm	$10^{-4}\ \varepsilon_5/M^{-1}\ cm^{-1}$	λ_6/nm	$10^{-4}\ \varepsilon_6/M^{-1}\ cm^{-1}$	λ_7/nm	$10^{-4}\ \varepsilon_7/M^{-1}\ cm^{-1}$
1	228	11	272	7.8	320	5.5	344 sh	4.2	466	1.8	—	—	—	—
2	222	7.1	246	6.6	280	7.8	308	7.6	344 sh	4.1	376	2.7	466	2.0
3	216	11	280	9.0	306	7.2	344 sh	4.0	374 sh	2.8	466	1.8	—	—
4	224	10	264	6.1	326	4.1	462	1.3	—	—	—	—	—	—

For [VO(sal-*L*-tryp)(phen)]•H_2O, ε_{710} = 29 M^{-1} cm^{-1} in DMSO.

[a]Complexes **1** and **2** were dissolved in 100% acetonitrile, while complexes **3** and **4** were dissolved in 2:1 MeOH/MeCN (v/v).

Table 2

ESR parameters for [VO(sal-*L*-tryp)(H_2O)], [VO(sal-*L*-tryp)(phen)]•H_2O, complex **3**, and complex **4**.

Complex	g_x	g_y	g_z	$10^4 A_x/cm^{-1}$	$10^4 A_y/cm^{-1}$	$10^4 A_z/cm^{-1}$	Ref.
[VO(sal-*L*-tryp)(H_2O)]	1.958	1.988	1.953	73	63	164	54
[VO(sal-*L*-tryp)(phen)]•H_2O	1.979	1.979	1.953	56.5	56.5	160.5	This work
3	1.978	1.978	1.954	56	56	162	This work
4	1.975	1.975	1.953	58	58	162	This work

[a] ESR parameters were obtained from spectral simulations as described in the text.

Table 3

ElectrOchemical data fOr [[VO(sal-*L*-tryp)(H_2O)], [VO(sal-*L*-tryp)(phen)•H_2O, [VO(sal-*L*-tryp)(MeATSC)•1.5C_2H_5OH, [VO(sal-*L*-tryp)(*N*-Ethriymethohcarbthio)]•H_2O, [VO(sal-*L*-tryp)(acetylethTSC)•C_2H_5OH, [Zn(sal-*L*-tryp)(H_2O)•0.25H_2O, and cOmplexes **1**–**4**.

Complex	$E_{1/2}$/V	Assignment	Reference
[VO(sal-*L*-tryp)(H_2O)][a]	E_{pa} = +0.71	*L*-trpy$^{0/+}$	55
	E_{pa} = +0.22	$V^{IV/V}$	
[VO(sal-*L*-tryp)(phen)]•H_2O[a]	E_{pa} = +0.39	$PhO^{-/\bullet}$	This wOrk
	E_{pa} = +0.20	$V^{IV/V}$	
[VO(sal-*L*-tryp)(MeATSC)]•1.5C_2H_5OH[a]	E_{pa} = +0.73	*L*-trpy$^{0/+}$	55
	E_{pa} = +0.21	$V^{IV/V}$	
[VO(sal-*L*-tryp)(*N*-EthhymethohcarbthioO]•H_2O[a]	E_{pa} = +0.64	*L*-trpy$^{0/+}$	55
	E_{pa} = +0.21	$V^{IV/V}$	
[VO(sal-*L*-tryp)(acetylethTSC)]•C_2H_5OH[a]	E_{pa} = +0.66	*L*-trpy$^{0/+}$	55
	E_{pa} = +0.21	$V^{IV/V}$	
[Zn(sal-*L*-tryp)(H_2O)]•0.25H_2O[a]	E_{pa} = +0.71	*L*-trpy$^{0/+}$	55
	E_{pa} = +0.59	$PhO^{-/\bullet}$	
1 [b]	+1.08	$Ru^{II/III}$	This wOrk
2 [b]	+1.12	$Ru^{II/III}$	This wOrk
3 [b]	+1.12	$Ru^{II/III}$	This wOrk
	E_{pa} = +0.93	*L*-trpy$^{0/+}$	
	E_{pa} = +0.55	$PhO^{-/\bullet}$	
	E_{pa} = +0.14	$V^{IV/V}$	
4 [a]	E_{pa} = +0.44	$PhO^{-/\bullet}$	This work
	E_{pa} = +0.21	$V^{IV/V}$	

[a]Recorded in DMSO

[b]Recorded in acetonitrile

Table 4

Anti-proliferative data obtained for the respective complexes in the presence of the various cell lines. Data are expressed as IC_{50} (μM). IC_{50} is defined as the concentration required to achieve 50% inhibition over control cells; IC_{50} values are shown as mean standard error values taken from three independent experiments.

Species	A431	HFF
$[Ru(pbt)_2(tpphz)VO(sal\text{-}L\text{-}tryp)]Cl_2$	41.3 ± 7.6	100.7 ± 17.7
$[Ru(pbt)_2(phen_2DTT)VO(sal\text{-}L\text{-}tryp)]Cl_2$	48.6 ± 13.1	204.4 ± 45.1
$[VO(sal\text{-}L\text{-}tryp)(phen)]\cdot H_2O$	41.6 ± 5.8	63.1 ± 28.3
$Na_4[Co(tspc)(H_2O)_2]$	>1000 but <2000	>2000
cisplatin	40.1 ± 11.5	82.0 ± 8.9